FISEVIER

Contents lists available at ScienceDirect

Mathematical Biosciences

journal homepage: www.elsevier.com/locate/mbs



Original Research Article

Dynamics of a predator–prey model with generalized Holling type functional response and mutual interference



Kwadwo Antwi-Fordjour a,*, Rana D. Parshad b, Matthew A. Beauregard c

- ^a Department of Mathematics and Computer Science, Samford University, Birmingham, AL 35229, USA
- ^b Department of Mathematics, Iowa State University, Ames, IA 50011, USA
- ^c Department of Mathematics and Statistics, Stephen F. Austin State University, Nacogdoches, TX 75962, USA

ARTICLE INFO

MSC:

34D45

37C10

37C75 37G15

92B05

Keywords:

Generalized interference Analytic guidelines

Finite time extinction

Hopf-bifurcation Prey refuge

ABSTRACT

Mutual interference and prey refuge are important drivers of predator-prey dynamics. The "exponent" or degree of mutual interference has been under much debate in theoretical ecology. In the present work, we investigate the interplay of the mutual interference exponent, and prey refuge, on the behavior of a predator-prey model with a generalized Holling type functional response — considering in particular the "non-smooth" case. This model can also be used to model an infectious disease where a susceptible population, moves to an infected class, after being infected by the disease. We investigate dynamical properties of the system and derive conditions for the occurrence of saddle-node, transcritical and Hopf-bifurcations. A sufficient condition for finite time extinction of the prey species has also been derived. In addition, we investigate the effect of a prey refuge on the population dynamics of the model and derive conditions such that the prey refuge would yield persistence of the population. We provide additional verification of our analytical results via numerical simulations. Our findings are in accordance with classical experimental results in ecology (Gause, 1934), that show that extinction of predator and prey populations is possible in a finite time period — but that bringing in refuge can effectively yield persistence.

1. Introduction

Predator–prey dynamics form the corner stone of ecosystems. Mathematical models for such interactions goes back to the work of Lotka, Volterra, Holling and Gause [1–4]. Holling's classical work proposes that a predator's feeding rate depends solely on the prey density, and is modeled essentially by a saturating function called the functional response, described via $p(x) = \frac{u(x)}{1+hu(x)}$, where h is the handling time of one prey item and u(x) is a function of prey density x. Typically u is smooth, making the response p smooth, and depending on the form of u we have Holling type II, III, IV responses [3,5]. The response, $p(x) = \frac{u(x)}{1+hu(x)}$, can be considered a special form of 2 different response types. $p(x) = \frac{(u(x))^p}{1+h(u(x))^p}$, or $p(x) = \left(\frac{u(x)}{1+hu(x)}\right)^{m_1}$. When p=1, or $m_1=1$, we recover the classical response posed earlier.

An interesting subclass of these general responses are the cases when $0 or <math>0 < m_1 < 1$. In these cases p(x) is non-smooth, causing various difficulties in the mathematical analysis of these systems. For example, linearization about the trivial steady state is no longer possible [6]. Such responses were considered by Sugie [6,7] and more recently by Braza [8]. Note, in these cases one might ask what real ecological scenarios do these models represent. The work by Sugie,

proposed the $(u(x))^p$ term, as indicative of a predator which is highly efficient and with a high attack rate. Such classes of models have also been considered in the more applied sense, where the focus has been on fitting similar functional responses, such as $(u(x))^p$, 0 , to actual predator–prey data [9,10]. However all of these works miss a key dynamic inherent in such models — that of finite time extinction of the prey. In fact [6,7] claim uniqueness of globally attracting interior equilibrium or limit cycle, under certain parametric restriction. This has recently been disproved in [11].

One might question the motivation behind studying finite time extinction in population dynamics. If we are modeling predator–prey numbers, once these quantities fall below one, populations are essentially extinct (and could also be deemed extinct due to inherent stochastic/environmental pressures). However, if we are modeling predator–prey densities, then a quantity less than one need not indicate essential extinction — and controls aimed at pest eradication if stopped at any finite time, would cause a rebound of the pest population [12]. Also, recent work on the Soybean aphid (*Aphis glicines*), the chief invasive pest on Soybean crop, particularly in the Midwestern US [13], shows that even the arrival of 20 soya bean aphid (where the density count is per leaf, so on an area ≈ 60 –70 cm²), is enough to overcome plant resistance and colonize the plant, reaching levels of several

E-mail address: kantwifo@samford.edu (K. Antwi-Fordjour).

^{*} Corresponding author.

thousand on one leaf, in a matter of 1-2 months. Herein the initial density would be $\approx 20/60 = \frac{1}{3} < 1$, and yet large scale invasion is possible [14].

Yet another powerful motivation to study finite time extinction comes from the vast epidemic literature. This is much in vogue, due to the ongoing global pandemic caused by the COVID19 virus [15]. In essence the models we analyze in the current manuscript, could be endemic models for an infectious disease due to which persons in a population transition from a susceptible state to an infected state, after being infected by the disease. The incidence function would be the density dependent rate at which this transition occurs. Recent work [16-18] has considered a large class of incidence functions, both upper density dependent incidence functions (these include density dependent incidence functions), Homogeneous incident functions (that include frequency dependent incidence) and power type incident functions (which are the ones under consideration in the current manuscript). Not only can power type incidence lead to host extinction in finite time — but are seen to be particularly good fits to modeling disease transmitted by rhanavirus among amphibian populations [19], modeling disease transmission among fairly general groups of hostparasitoid models [20], as well as in modeling virus transmission in gypsy moths [21].

Mathematically, this is made possible, due to the "non-smooth" form of the responses considered, where by the stable manifold of the origin, separates the phase space into initial conditions that could result in finite time extinction of prey, followed by an exponential decrease of predators also to extinction — versus initial conditions that could possibly go to an interior equilibrium or some other closed loop in the phase space, such as a heteroclinic orbit or limit cycle. Such a separation in the phase has been seen in the predator-prey literature, but this has almost exclusively been in the Leslie-Gower type models, where the predator nullcline is slanting and not vertical, see [22] and the references within. It has also been seen via introduction of Allee effects, see [23-26] and the references within. However, in the nonsmooth case, as first considered in [6,7,9], a careful analysis of this splitting of phase, initial condition dependent extinction, and all of the rich dynamics and bifurcations involved therein, have only been considered in [11], to the best of our knowledge. However, studying non-smooth form of the responses, as in the applications alluded to in the present work, provides insight into various ecological and epidemic processes, all of which occur in finite time.

Mutual interference is defined as the behavioral interactions among feeding organisms, that reduce the time that each individual spends obtaining food, or the amount of food each individual consumes [27-32]. Some of the earliest work on mutual/predator interference, was initiated by Erbe [33], in which the mutual interference is modeled as $\frac{u(x)}{1+hu(x)}y^m$, where y is the predator density and 0 < m < 1. The exact Various authors describe the response $p(x) = \left(\frac{u(x)}{1 + hu(x)}\right)^{m_1}$ in terms of mutual interference. This direction was first considered by Upadhyay and Rao [35]. However, an ecological motivation, to the best of our knowledge is not provided. We are motivated by certain theoretical ecology directions [32,36–38], and interpret $p(x) = \left(\frac{u(x)}{1+hu(x)}\right)^{m_1}$, 0 < $m_1 < 1$, as a predator with a greater feeding rate, or a more aggressive predator, than one which is modeled in the classical scenario — that is when $m_1 = 1$. This is clear from simple comparison, $p(x)|_{m_1=1}$ $p(x)|_{0 < m_1 < 1}, \ \forall x > 0.$

Prey refuge, and its role in predator-prey communities has also been extremely well investigated, since the seminal work of Kar [39]. Refuge is defined as any strategy taken by prey to avoid predation, such as shelter, dispersal, mimicry and camouflage [40]. It can have strong influence on predator-prey communities [41,42] — often stabilizing systems, which are otherwise doomed for extinction. It is thus an important ingredient in ecosystem balance and diversity [43]. However, the effect of refuge on non-smooth systems such as the aforementioned ones, remains less investigated [43]. The well known experiments of Gause find in contradiction to the predictions of classical predatorprev models, that there is a distinct chance for the predator and prev populations to die out — unless the prey is provided with refuge [2]. Non-smooth systems such as when $0 < m, m_1 < 1$, in the aforementioned models, enable the dynamic of finite time predator-prey extinction (such as seen in the experiments of Gause [2,42]) — however, to the best of our knowledge, the effect of prey refuge on these systems has not been investigated.

For the purposes of this manuscript we consider the functional response $p(x) = \left(\frac{u(x)}{1+hu(x)}\right)^{m_1}$, and define the parameter regimes $m_1 > 1$ as super-critical, that is the regime where $p(x) \in C^k$, $\forall k$, and u(x) is a polynomial function. We define $m_1 = 1$ as *critical*, recovering the classical case from the literature. Lastly we define $0 < m_1 < 1$ as sub*critical*, that is the regime where p(x) loses smoothness, and is not even Lipschitz. Thus the goals of the current manuscript are:

- (1) To consider a generalized model of interference, in the subcritical regime; therein to investigate the phenomenon of finite time prey extinction, that can occur in this regime. This is seen via Theorems 4.1 and 4.2.
- (2) To investigate this model dynamically, including the various bifurcations that might occur. These are visualized through
- (3) To investigate the effect of prey refuge on the dynamics of this generalized model. We find that there is a critical amount of refuge that prevents finite time extinction of the prey. This is seen via Theorem 5.1.

The rest of the paper is organized as follows. The mathematical formulation of the problem and mathematical preliminaries such as nonnegativity, boundedness and dissipativeness are presented in Section 2. Analytic guidelines and various local bifurcations are considered in Section 3. In Section 4, we analyze the possibility of finite time extinction of the prey population. We investigate the effect of prey refuge in Section 5. Additionally, analytic guidelines and various local bifurcations are carried out. Numerical simulations are performed in various sections to correlate with our key analytical findings. In the last section, we present our discussions and conclusions. We have included several technical Appendices A and B.

2. Model formulation

First, we consider a general predator-prey model with mutual interference among predators of the form

$$\begin{cases} \frac{dx_1}{dt} &= x_1 f(x_1) - w_0 g(x_1) x_2^{m_2}, \\ \frac{dx_2}{dt} &= -a_2 x_2 + w_1 g(x_1) x_2^{m_2}, \end{cases}$$
(1)

where $f(x_1)$ and $g(x_1)$ are the logistic growth and the functional response of the predator towards the prey respectively. Assume that $0 < m_2 \le 1$, as per literature on mutual interference [27,28]. In this paper, we consider the general logistic growth and the generalized Holling type functional response, see [44,45]:

$$f(x) = a_1 - b_1 x, \qquad g(x) = \left(\frac{x}{x+d}\right)^{m_1}.$$
 (2)

Assume that $0 < m_1 \le 1$. The assumptions placed on the functions fand g in (2) are:

- (I) g is continuous for $x_1 \ge 0$ and g(0) = 0;
- (II) g is smooth for $x_1 > 0$ and $g'(x_1) > 0$ for $x_1 > 0$;
- (III) f is smooth for $x_1 \ge 0$; (IV) There exists $\frac{a_1}{b_1} > 0$ such that $\left(x_1 \frac{a_1}{b_1}\right) f(x_1) < 0$ for $x_1 \ge 0$, $x_1 \ne \frac{a_1}{L}$;
- (V) For $0 < m_1 < 1$, $g'(0^+) := \lim_{x_1 \to 0^+} \frac{g(x_1)}{x_1} = +\infty$;

Table 1
List of parameters used in the model (3). All parameters considered are positive constants.

Variables/	Description			
Parameters				
x_1	Prey population			
x_2	Predator population			
t	Time			
a_1	Per capita rate of self-reproduction for the prey			
a_2	Intrinsic death rate of the predator population			
w_0	Maximum rate of per capita removal of prey			
w_1	Measure efficiency of biomass conversion from prey to predator			
b_1	Death rate of prey population due to intra-species competition			
d	Half saturation constant			
$1/m_1$	Predators feeding intensity			
m_2	Mutual interference exponent			

(VI)
$$g$$
 is not smooth for $x_1=0$ when $0< m_1<1$; (VII) The integral $\lim_{\epsilon\to 0}\int_{\epsilon}^{\beta}\frac{dx_1}{g(x_1)}$ converges for fixed $\beta>0$.

Thus the predator-prey model with mutual interference and the generalized Holling type functional response becomes

$$\begin{cases} \frac{dx_1}{dt} &= a_1 x_1 - b_1 x_1^2 - w_0 \left(\frac{x_1}{x_1 + d}\right)^{m_1} x_2^{m_2}, \\ \frac{dx_2}{dt} &= -a_2 x_2 + w_1 \left(\frac{x_1}{x_1 + d}\right)^{m_1} x_2^{m_2}, \end{cases}$$
(3)

The variables and parameters used in the model are defined in Table 1.

2.1. Mathematical preliminaries

There are essential properties that a mathematical model must exhibit in order to obtain realistic solutions. In particular, it is important to guarantee positivity of the populations. Likewise, boundedness of the total population is another important feature of a realistic model. In this section, we show positivity, boundedness, and dissipativeness of the mathematical model (3).

2.1.1. Positivity and boundedness

The nonnegativity of populations generated by the mathematical model (3) is clearly important to make biological sense. In addition, positivity implies survival of the populations over the temporal domain. The boundedness of populations ensures that no population supersedes unrealistic values in time. In particular, boundedness guarantees that the total population does not grow beyond an exponential rate for an unbounded interval. Guaranteeing both of these features makes strides to showing the feasibility of a mathematical model for describing population behavior.

Lemma 2.1. Consider the following region $\mathbb{R}^2_+ = \{(x_1, x_2) : x_1 \ge 0, x_2 \ge 0\}$, then all solutions $(x_1(t), x_2(t))$ of model (3) with initial conditions $x_1(0) > 0$, $x_2(0) > 0$ are nonnegative for all $t \ge 0$.

Proof. The proof of Lemma 2.1 follows from the proof of Theorem 3.1 in [44]. \Box

Remark 1. In fact, x_2 remains positive for all t > 0. Due to the property of finite time prey extinction (see Theorem 4.1, Theorem 4.2) the predator population x_2 could approach 0, but only asymptotically, that is in infinite time.

Lemma 2.2. All solutions $(x_1(t), x_2(t))$ of model (3) with initial conditions $x_1(0) > 0$, $x_2(0) > 0$ are bounded.

Proof. Let us define the function $Q(x_1(t), x_2(t)) = x_1(t) + x_2(t)$. Then

$$\frac{dQ}{dt} = \frac{ax_1}{dt} + \frac{ax_2}{dt} \qquad \text{where } K_1 = (a_1 + a_2) \left(\frac{1}{b_1} + a_2\right) \left(\frac{1}{b_1} + a_$$

Let δ be a positive constant such that $\delta \leq a_2$ and suppose $w_0 \geq w_1$, then we obtain,

$$\begin{split} \frac{dQ}{dt} + \delta Q &= a_1 x_1 - b_1 x_1^2 - w_0 \left(\frac{x_1}{x_1 + d}\right)^{m_1} x_2^{m_2} \\ &- a_2 x_2 + w_1 \left(\frac{x_1}{x_1 + d}\right)^{m_1} x_2^{m_2} + \delta(x_1 + x_2) \\ &= a_1 x_1 - b_1 x_1^2 - (w_0 - w_1) \left(\frac{x_1}{x_1 + d}\right)^{m_1} x_2^{m_2} - (a_2 - \delta) x_2 + \delta x_1 \\ &\leq (a_1 + \delta) x_1 - b_1 x_1^2 \leq \frac{(a_1 + \delta)^2}{4b_1}. \end{split}$$

Taking $W_1 = \frac{(a_1 + \delta)^2}{4b_1}$ and applying the theory on differential inequality, we obtain

$$0 \le Q\left(x_1(t), x_2(t)\right) \le \frac{W_1(1 - e^{-\delta t})}{\delta} + Q\left(x_1(0), x_2(0)\right) e^{-\delta t}.$$

which implies

$$\lim_{t \to \infty} \sup Q\left(x_1(t), x_2(t)\right) \le \frac{W_1}{\delta}.\tag{4}$$

By (4) and Lemma 2.1, all solutions of (3) with initial conditions $x_1(0) > 0$, $x_2(0) > 0$ will be contained in the region

$$\Theta = \{(x_1, x_2) \in \mathbb{R}^2_+ : Q\left(x_1(t), x_2(t)\right) \le \frac{W_1}{\delta} + \epsilon, \text{ for any } \epsilon > 0\}.$$

The proof is complete. \square

2.1.2. Dissipativeness

In the previous section, it was shown that the total population remains positive and bounded for all time. Here, we showed that the individual populations are all bounded from above. In such a situation, we say that the model is dissipative.

Lemma 2.3. The system (3) is dissipative.

Proof. From the first system of (3)

$$\begin{split} \frac{dx_1}{dt} &= a_1 x_1 - b_1 x_1^2 - w_0 \left(\frac{x_1}{x_1 + d}\right)^{m_1} x_2^{m_2}, \\ &\leq a_1 x_1 - b_1 x_1^2. \end{split}$$

This implies that

$$\lim_{t \to \infty} \sup x_1(t) \le \frac{a_1}{b_1}.\tag{5}$$

The inequality (5) gives that for arbitrary small $\epsilon_1>0$, there exists a real number T>0 such that

$$x_1(t) \le \frac{a_1}{b_1} + \epsilon_1$$
, for all $t \ge T_1$. (6)

Using (6), we obtain for all $t \ge T_1$,

$$\begin{split} \frac{d}{dt}\left(x_1 + \frac{w_0 x_2}{w_1}\right) &= \frac{dx_1}{dt} + \frac{w_0}{w_1} \frac{dx_2}{dt} \\ &= a_1 x_1 - b_1 x_1^2 - \frac{w_0 a_2}{w_1} x_2 \\ &\leq a_1 x_1 - \frac{w_0 a_2}{w_1} x_2 \\ &= (a_1 + a_2) x_1 - a_2 \left(x_1 + \frac{w_0 x_2}{w_1}\right) \\ &\leq K_1 - a_2 \left(x_1 + \frac{w_0 x_2}{w_1}\right), \end{split}$$

where $K_1 = (a_1 + a_2) \left(\frac{a_1}{b_1} + \epsilon_1 \right)$. Therefore, we obtain

$$\limsup_{t \to \infty} \left(x_1 + \frac{w_0 x_2}{w_1} \right) \le \frac{K_2}{a_2}. \tag{7}$$

By (5) and (7), there exists a real number K_2 such that

$$\limsup_{t\to\infty} x_2 \le K_2.$$

Thus, for arbitrary small $\epsilon_2 > 0$, there exists $T_2 > T_1 > 0$, such that for all $t \geq T_2$

$$x_2 \leq K_2 + \epsilon_2$$
.

Therefore the model (3) is dissipative.

3. Analytic guidelines

In this section, we present analytic guidelines to investigate equilibria for our mathematical model. Consider the solutions to the steady state equations:

$$a_1 x_1 - b_1 x_1^2 - w_0 \left(\frac{x_1}{x_1 + d}\right)^{m_1} x_2^{m_2} = 0$$
 (8)

$$-a_2x_2 + w_1 \left(\frac{x_1}{x_1 + d}\right)^{m_1} x_2^{m_2} = 0$$
(9)

The above equations, (8) and (9), have three types of non-negative equilibria:

- (i) The trivial equilibrium $E_0(0,0)$;
- (ii) The predator-free equilibrium $E_1(a_1/b_1, 0)$;
- (iii) The interior equilibrium $E_2(x_1^*, x_2^*)$ where x_1^* and x_2^* are related

$$x_2^* = \frac{w_1}{w_0 a_2} \left[a_1 x_1^* - b_1 x_1^{*2} \right].$$

We have that $a_1 - b_1 x_1^* \ge 0$ since $x_1^* \ge 0$ and $x_2^* \ge 0$. The possible existence of a unique or multiple interior equilibria is shown in Fig. 1.

Remark 2. We focus on the case where $m_2 = 1$ and assumptions (V)–(VII) hold, then E_0 is a saddle point, but standard linear stability arguments cannot be applied, as our response function g is not Lipschitz at the origin. We will describe the global behavior of the system (3) by considering the relative position of the stable and unstable separatrix of the saddle points E_0 and E_1 respectively. We denote the stable manifold of E_0 by $W^s(E_0)$ and the unstable manifold of E_1 by $W^u(E_1)$.

The predator nullcline is the vertical line $x_1 = x_1^*$ determined by the equation $-a_2 + w_1 g(x_1) = 0$. We assume

$$w_1 > a_2, \qquad \frac{a_1}{b_1} > x_1^* := \frac{d \ a_2^{\frac{1}{m_1}}}{w_1^{\frac{1}{m_1}} - a_2^{\frac{1}{m_1}}}.$$
 (10)

The prey nullcline is the graph of the function $y = \psi(x_1)$

$$\psi(x_1) = \frac{x_1 f(x_1)}{w_0 g(x_1)} \tag{11}$$

where $f(x_1)$ and $g(x_1)$ are defined in (2). Clearly $\psi(\frac{a_1}{b_1}) = 0$ and $\psi(x_1) > 0$ 0 for $0 < x_1 < \frac{a_1}{b_1}$. The unique interior equilibrium $E_2(x_1^*, x_2^*)$ is the intersection of the predator and prey nullclines and it can be stable or unstable depending on the sign of $\psi'(x_1^*)$. For $\psi'(x_1^*) > 0$, E_2 is a repeller and for $\psi'(x_1^*) < 0$, E_2 is locally asymptotically stable.

Remark 3. The predator-free equilibrium E_1 turns into a stable node with the loss of the unique interior equilibrium E_2 . Herein, the vertical nullcline would have to move to the right of the predator-free equilibrium E_1 .

Remark 4. The interior equilibrium E_2 is always unique. However, in our system we have non-uniqueness of solutions when $m_1 < 1$. Here we mean non-uniqueness backwards in time. Essentially the x_2 axis, consists of all non-uniqueness points, see Theorem 2.1 in [11] for details.

We now present the following results that pertain to the dynamics of (3), when $0 < m_1 < 1, m_2 = 1$.

Lemma 3.1. Assume that $W^s(E_0)$ is above $W^u(E_1)$. If E_2 is a repeller, then it is surrounded by at least one limit cycle. If the system can have at most one cycle, then E_2 is surrounded by at least a unique limit cycle which is orbitally asymptotically stable. This limit cycle is not globally orbitally asymptotically stable, even if it is unique. If E_2 is locally asymptotically stable and if the system has no cycles, then all orbits under $W^s(E_0)$ converge towards E_2 . E_2 is not globally asymptotically stable, even if it is not surrounded by any unstable limit cycle.

Proposition 3.2. Assume $\psi'(x_1^*) \leq 0$ and (10) hold, then $W^s(E_0)$ is above $W^{u}(E_1)$ and the basin of attraction of E_2 is the positive region of the plane located under $W^s(E_0)$. Hence E_2 is not globally asymptotically stable.

The proofs of the above follow the proofs of Proposition 3.1 and Proposition 4.2 in [11], and omitted for brevity.

3.1. Saddle-node bifurcation

We investigate the possibility of saddle-node bifurcation of the positive interior equilibrium E_2 by using the intrinsic death rate of the predator population as a bifurcation parameter.

Let J^* denote the variational matrix of the model (3) around an interior equilibrium $E_2(x_1^*, x_2^*)$. The following theorem states the restrictions for occurrence of a saddle-node bifurcation for model (3).

Theorem 3.3. The model (3) undergoes a saddle–node bifurcation around E_2 at a_2^* when the system parameters satisfy the restriction det $(\mathbf{J}^*) = 0$ along with the condition $\operatorname{tr}(\mathbf{J}^*) < 0$.

3.2. Hopf-bifurcation

We investigate the possibility of Hopf-bifurcation of the positive interior equilibrium E_2 by using the per capita rate of self-reproduction for the prey, a_1 as a bifurcation parameter. Then, the characteristic equation corresponding to model (3) at E_2 is given by

$$\lambda^2 + A(a_1)\lambda + B(a_1) = 0, (12)$$

where $A = -\operatorname{tr}(\mathbf{J}^*) = -(a_{11} + a_{22})$ and $B = \det(\mathbf{J}^*) = a_{11}a_{22} - a_{12}a_{21}$.

The instability of model (3) is demonstrated via the following theorem by considering a_1 as a bifurcation parameter.

Theorem 3.4 (Hopf-bifurcation Theorem [46]). If $A(a_1)$ and $B(a_1)$ are the smooth functions of a_1 in an open interval about $a_1^* \in \mathbb{R}$ such that the characteristic equation (12) has a pair of imaginary eigenvalues λ = $\zeta(a_1) \pm i \gamma(a_1)$ with ζ and $\gamma \in \mathbb{R}$ so that they become purely imaginary at $a_1=a_1^*$ and $\frac{d\zeta}{da_1}|_{a_1=a_1^*}\neq 0$, then a Hopf-bifurcation occurs around $E_2(x_1^*,x_2^*)$ at $a_1=a_1^*$ (i.e. a stability changes of $E_2(x_1^*,x_2^*)$ accompanied by the creation of a limit cycle at $a_1 = a_1^*$).

Theorem 3.5. The model (3) undergoes a Hopf-bifurcation around $E_2(x_1^*, x_2^*)$ when a_1 crosses some critical value of parameter a_1^* , where

$$a_1^* = a_2 + 2b_1x_1^* - m_2w_1x_2^{*m_2-1} \left(\frac{x_1^*}{x_1^* + d}\right)^{m_1} + dm_1w_0x_2^{*m_2} \left(\frac{x_1^{*m_1-1}}{(x_1^* + d)^{m_1+1}}\right)$$

provided:

- (i) $A(a_1) = 0$,

$$\begin{array}{ll} \mbox{(ii)} & B(a_1) > 0, \\ \mbox{(iii)} & \frac{d}{da_1} \left. Re \lambda_i(a_1) \right|_{a_1 = a_1^*} \neq 0 \mbox{ at } a_1 = a_1^*, \ i = 1, 2. \end{array}$$

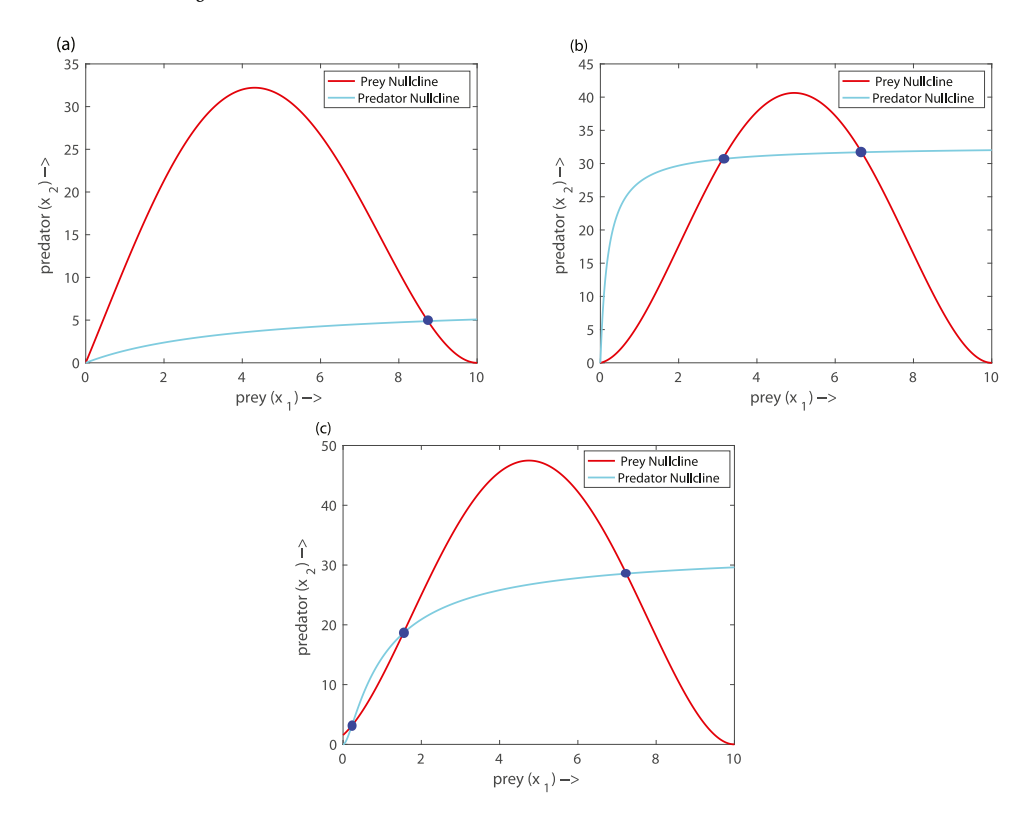


Fig. 1. Figure (a) and (b) represent graphical illustration of the predator and prey non-trivial nullclines when $m_1 = m_2 = 0.5$. Figure (c) represents graphical illustration of the predator and prey non-trivial nullclines when $m_1 = 1$, $m_2 = 0.5$.

Table 2Parameters used in the simulations of Figs. 2–4 and 6–8.

$a_1 = 0.6$	$a_2 = 1$	$b_1 = 0.063$	$w_0 = 1$	d = 2
$w_1 = 2$	$w_2 = 1$	$w_3 = 2$	$m_1 = 0.8$	$m_2 = 1$

Parameters used in the simulations of Figs. 5, 9 and 10.

$a_1 = 0.5$	$a_2 = 0.7$	$b_1 = 0.05$	$w_0 = 0.2$	d = 0.2
$w_1 = 4$	$w_2 = 0.2$	$w_3 = 4$	$m_1 = 0.5$	$m_2 = 0.5$

3.3. Numerical simulations

Based on the analytical guidelines we have presented earlier we now showcase some numerical simulations of model (3), to correlate with the earlier guidelines. The numerical simulations and figures have been developed using MATLAB®R2019b, MATCONT [47], and XPPAUT [48]. For convenience, the parameters used in simulations are given in Tables 2 and 3.

In Fig. 2(a), $W^s(E_0)$ is above $W^u(E_1)$ and $E_2(1.45094, 1.0299)$ is surrounded by a unique limit cycle. This unique limit cycle attracts all orbits under $W^s(E_0)$. It is seen that in Fig. 2(b), $W^s(E_0)$ is under $W^u(E_1)$. The predator-free equilibrium point $E_1(9.52381,0)$ is a saddle and $E_2(1.45094, 4.91957)$ is unstable. Here all positive solutions converge towards E_0 .

In Fig. 3(a), we observe that $E_2(3.55994,4.36963)$ is locally asymptotically stable and $E_1(8.33333,0)$ is a saddle. Also $W^s(E_0)$ is above $W^u(E_1)$ and the basin of attraction is the region under $W^s(E_0)$. However, in this figure, the numerical simulations illustrate that E_2 is not globally asymptotically stable for the given parameter set. In Fig. 3(b), $E_2(1.45094,1.47966)$ is unstable and we obtain a heteroclinic bifurcation when $W^u(E_1) = W^s(E_0)$ for $0.062 < b_1 < 0.063$.

Furthermore, for the parameter sets in Table 2, we employ AUTO as implemented in the continuation software XPPAUT to analyze the bifurcation diagrams of the model (3) in Fig. 4. The model undergoes Hopf-bifurcation around $E_2(1.45094, 0.49456)$ as the parameter a_1 crosses its critical value $a_1^*=0.261835$. The branch of periodic orbits emitting from a_1^* is stable and the first Lyapunov coefficient [49], $\sigma=-1.49929e^{-2}<0$ (obtained with the aid of MATCONT), hence the Hopf-bifurcation is supercritical.

We observed that the model (3) undergoes a saddle–node bifurcation around $E_2(x_1^*, x_2^*)$ when the parameter a_1 crosses their corresponding critical values $a_1^* = 0.46809$. The saddle–node bifurcation diagram is depicted in Fig. 5

4. Finite time extinction

An interesting property of (3) is that the prey population can go extinct in finite time for certain initial conditions, and so although solutions remain nonnegative, they may go to the extinction state and not persist. We state and prove the following result.

Theorem 4.1. Consider the predator–prey system given by (3). The solution $x_1(t)$ to the prey equation $x_1(t)$ with initial conditions $x_1(0) > 0$, $x_2(0) > 0$ will go extinct in finite time, for $x_1(0)$ chosen sufficiently small and $x_2(0)$ chosen sufficiently large.

Proof. Consider the substitution $x_1 = 1/u$ in the prey equation of (3). This yields the following system:

$$\begin{cases} \frac{dx_1}{dt} = \frac{-1}{u^2} \frac{du}{dt} &= a_1 \frac{1}{u} - b_1 \left(\frac{1}{u}\right)^2 - w_0 \left(\frac{\frac{1}{u}}{\frac{1}{u} + d}\right)^{m_1} x_2^{m_2}, \\ \frac{dx_2}{dt} &= -a_2 x_2 + w_1 \left(\frac{\frac{1}{u}}{\frac{1}{u} + d}\right)^{m_1} x_2^{m_2}. \end{cases}$$
(13)

This system can be simplified into the system in u, x_2 :

$$\begin{cases} \frac{du}{dt} = -a_1 u + b_1 + w_0 \frac{u^2}{(1+du)^{m_1}} x_2^{m_2}, \\ \frac{dx_2}{dt} = -a_2 x_2 + w_1 \frac{1}{(1+du)^{m_1}} x_2^{m_2}, \end{cases}$$
(14)

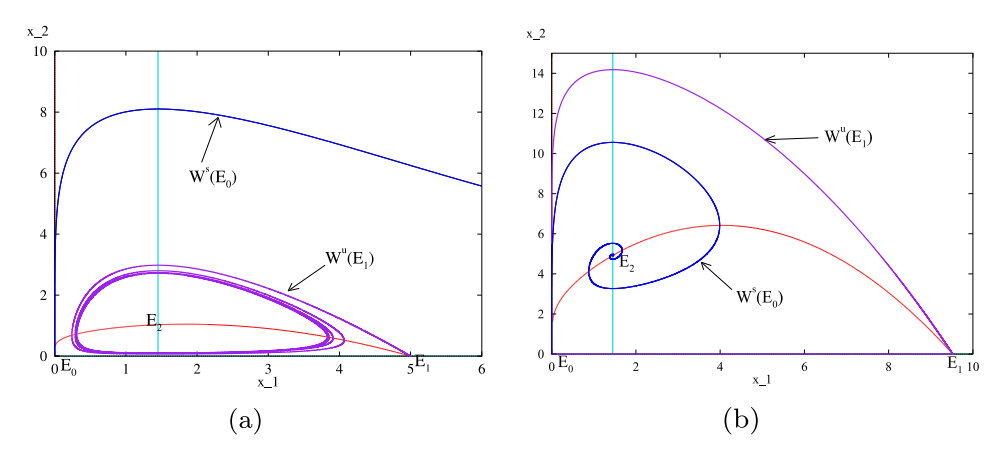


Fig. 2. The predator and prey nullclines for model (3) are represented by turquoise and red respectively. (a) $W^{s}(E_{0})$ is above $W^{u}(E_{1})$: E_{2} is unstable. Here $a_{1} = 0.5$ and $b_{1} = 0.1$ (b) $W^{u}(E_{1})$ is above $W^{s}(E_{0})$, here $a_{1} = 2$ and $b_{1} = 0.21$: E_{2} is unstable. Other parameter sets are given in Table 2.

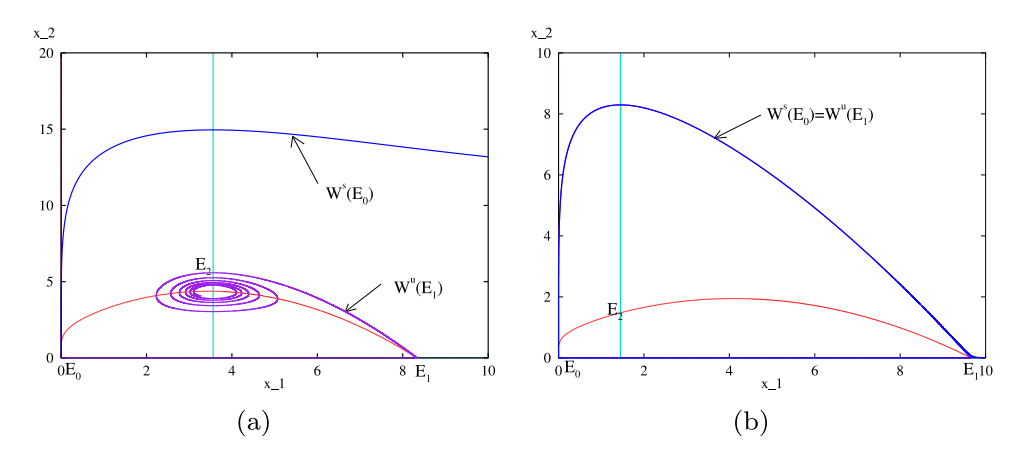


Fig. 3. (a) E_2 is a locally asymptotically stable and $W^s(E_0)$ is above $W^u(E_1)$. Here $a_1 = 1.5$, $b_1 = 0.18$ and $a_2 = 1.4$. (b) E_2 is unstable and $W^u(E_1) = W^s(E_0)$. Here $0.062 < b_1 < 0.063$. Other parameter sets are given in Table 2.

Note, via positivity

$$\frac{dx_2}{dt} \ge -a_2 x_2. \tag{15}$$

Thus,

$$x_2 \ge x_2(0)e^{-a_2t}. (16)$$

Also, via positivity we have the inequality,

$$\frac{du}{dt} \geq -a_1 u + w_0 \frac{u^2}{(1+du)^{m_1}} x_2^{m_2} \geq -a_1 u + w_0 \frac{u^2}{(1+du)^{m_1}} (x_2(0) e^{-a_2 t})^{m_2}. \tag{17}$$

Note that the solution to the differential equation

$$\frac{d\tilde{u}}{dt} \ge -a_1 \tilde{u} + w_0 \frac{\tilde{u}^2}{(1 + d\tilde{u})^{m_1}} \tag{18}$$

will blow up in a finite time, $T^*(u_0) < \infty$, as long as the initial data $\tilde{u}(0) = u_0$ satisfies,

$$a_1 u_0 (1 + du_0)^{m_1} \le w_0 u_0^2. (19)$$

Now if we choose $x_2(0) \gg 1$, such that

$$(x_2(0)e^{-a_2t})^{m_2} > 1, \ t \in [0, T^*], \tag{20}$$

then $u \ge \tilde{u}$ on $[0, T^*]$, and must blow-up in finite time, at some $T^{**} < T^*$, by comparison, if u_0 is chosen to satisfy (19). Therefore,

$$\lim_{t \to T^{**} < \infty} u \to \infty$$

which implies

$$\lim_{t \to T^{**} < \infty} x_1 = \lim_{t \to T^{**} < \infty} \frac{1}{u} = \frac{1}{\lim_{t \to T^{**} < \infty} u} \to 0,$$

but that implies $x_1(t)$ goes extinct in finite time for $x_2(0)$ chosen large enough and

$$(x_1(0))^{1-m_1}(x_1(0)+d)^{m_1} \le \frac{w_0}{a_0}.$$

We now state and prove a stronger result than Theorem 4.1, following methods in [17],

Theorem 4.2. Consider the predator–prey system given by (3). The solution $x_1(t)$ to the prey equation will go extinct in finite time, for initial conditions chosen s.t. $1 \le x_1(0) \le \frac{a_1}{b_1}$, $g_1(x_1(0)) \le (x_2(0))^{m_2}$, where g_1 is chosen via (28).

Proof. Consider the prey equation for initial condition $1 \le x_1(0) \le \frac{a_1}{b_1}$.

$$\frac{dx_1}{dt} \le a_1 x_1 - b_1 x_1^2,\tag{21}$$

thus $x_1(t) \le \frac{a_1}{b_1}$, for all time t>0. This follows via comparison of the prey equation above, to the logistic equation. Next,

$$\frac{dx_1}{dt} = a_1 x_1 - b_1 x_1^2 - w_0 \left(\frac{x_1}{x_1 + d}\right)^{m_1} x_2^{m_2}
\leq a_1 x_1 - b_1 x_1^2 - w_0 \left(\frac{1}{\frac{a_1}{b_1} + d}\right)^{m_1} (x_2(0))^{m_2} e^{-m_2 a_2 t} (x_1)^{m_1}
\leq a_1 x_1 - w_0 \left(\frac{1}{\frac{a_1}{b_1} + d}\right)^{m_1} (x_2(0))^{m_2} e^{-m_2 a_2 t} (x_1)^{m_1}$$
(22)

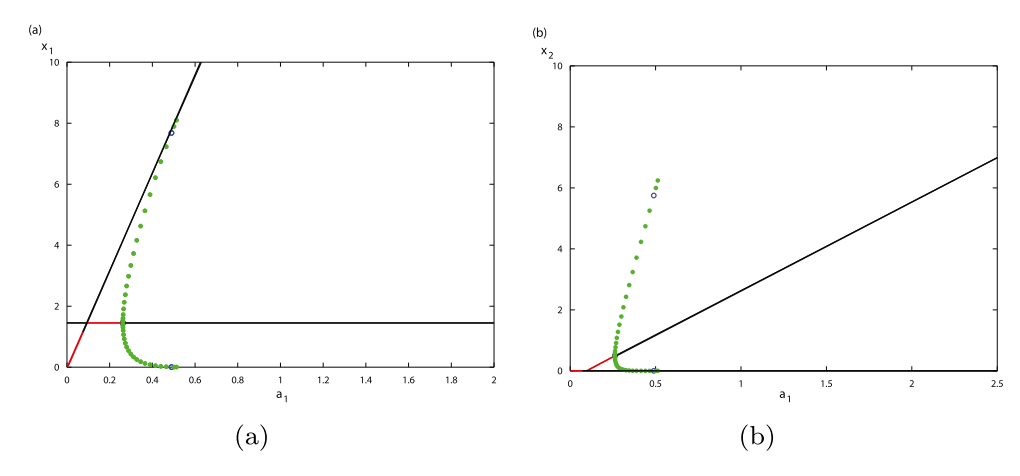


Fig. 4. Bifurcation diagrams of the model (3), as a_1 changes. The stable and unstable interior equilibria are given by the lines in red and black, respectively. The solid circles (green) represent stable limit cycles and the open circles (blue) represent unstable limit cycles. (a) prey (x_1) (b) predator (x_2) . Parameter sets are given in Table 2.

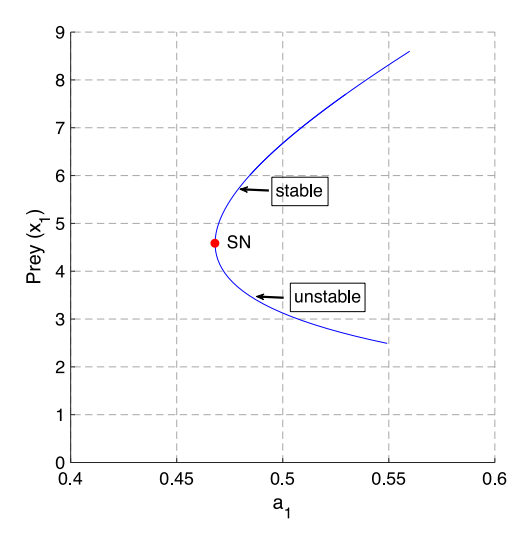


Fig. 5. Bifurcation diagrams illustrating SN at $a_1 = a_1^* = 0.46809$. Other parameter sets are given in Table 3. (SN: Saddle–node bifurcation.)

This follows via the comparison $\frac{dx_2}{dt} \ge -a_2x_2$, and the form of the functional response. Now we can divide the above by $(x_1)^l$, where $l \le m_1$, will be chosen a posteriori, to obtain,

$$\frac{dx_1}{dt} \frac{1}{(x_1)^l} \le a_1 x_1^{1-l} - w_0 \left(\frac{1}{\frac{a_1}{b_1} + d} \right)^{m_1} (x_2(0))^{m_2} e^{-m_2 a_2 t} (x_1)^{m_1 - l}$$
 (23)

this yields

$$\frac{d}{dt}((x_1)^{1-l}) \leq (1-l)a_1(x_1)^{1-l} - (1-l)w_0 \left(\frac{1}{\frac{a_1}{b_1} + d}\right)^{m_1} (x_2(0))^{m_2} e^{-m_2 a_2 t} \eqno(24)$$

This follows since if $x_1(0) > 1$ then $x_1 \ge 1$ at least on some time interval $[0, T^*]$. Now following [17], multiplying both sides by the integrating factor $e^{-(1-l)a_1t}$ yields,

$$\frac{d}{dt}(e^{-(1-l)a_1t}(x_1)^{1-l}) \le -(1-l)w_0 \left(\frac{1}{\frac{a_1}{b_1}+d}\right)^{m_1} (x_2(0))^{m_2} e^{-m_2 a_2 t} e^{-(1-l)a_1 t}$$
(25)

We integrate the above in the time interval [0,t] with $t \leq T^*$ to obtain

$$e^{-(1-l)a_1t}(x_1)^{1-l}$$

$$\leq (x_1(0))^{1-l} - w_0 \left(\frac{(1-l)\left(\frac{1}{\frac{a_1}{b_1} + d}\right)^{m_1} (x_2(0))^{m_2}}{a_2 m_2 + (1-l)a_1} \right) (1 - e^{-(a_2 m_2 + (1-l)a_1)t})$$
 (26)

which then implies the finite time extinction of x_1 , if

$$(x_1(0))^{1-l} < w_0 \left(\frac{(1-l)\left(\frac{1}{\frac{a_1}{b_1}+d}\right)^{m_1} (x_2(0))^{m_2}}{a_2m_2 + (1-l)a_1} \right)$$
(27)

Thus we choose g_1 according to

$$g_1(x_1(0)) = \left(\frac{a_2 m_2 + (1 - l)a_1}{w_0(1 - l)\left(\frac{1}{b_1} + d\right)^{m_1}}\right) (x_1(0))^{1 - l}$$
(28)

and for initial data chosen s.t $(x_2(0))^{m_2} \ge g_1(x_1(0))$, x_1 will go extinct in finite time. \square

Remark 5. From [17] we know that the initial data needs to be chosen s.f.

to yield finite time extinction of x_1 . Our construction allows us to choose l s.t the curve g_1 , will be no higher than in (29), as derived in [17] (but possibly lower). Note, from the analytic guidelines and simulations of Section 3, we see that the equilibrium $E_0=(0,0)$, always exists and is a saddle. Thus there exists a stable manifold/separatrix, which we denote $W^s(E_0)$ that divides the phase space into two regions. If we are above $W^s(E_0)$, initial data hits the y-axis in finite time, and then approaches (0,0) asymptotically. If we are below $W^s(E_0)$ then the data may go to the interior equilibrium, or cycle, or go to predator free equilibrium. Thus one needs to ensure g_1 lies above $W^s(E_0)$. If g_1 went below $W^s(E_0)$, trajectories may be attracted to E_1 or a limit cycle surrounding E_1 , and finite time extinction of x_1 would not occur. See Fig. 6(c).

We provide some simulations next to elucidate.

Next, we state a result, that has to do with a functional response which may depend on both the prey and predator. These include

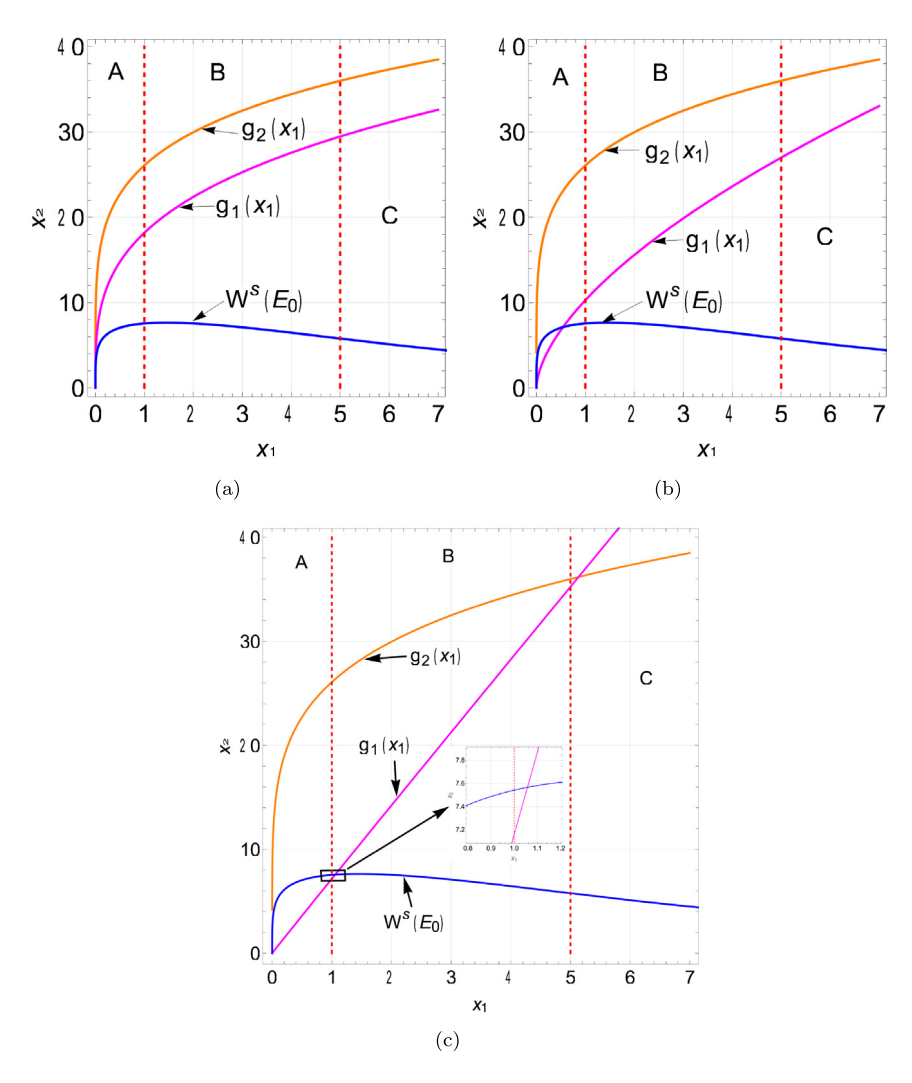


Fig. 6. Herein we demonstrate our result from Theorem 4.2. In the simulations, g_2 is the curve predicted via [17], s.t. if we are above g_2 , we see finite time extinction. However, choosing $l < m_1 = 0.8$, we derive a curve given by g_1 . In (a) l = 0.7, (b) l = 0.4 and (c) l = 0.01. Here $a_1 = 0.5$, $b_1 = 0.1$, and all other parameter sets are given in Table 2. Notice in (b), g_1 dips below $W^s(E_0)$ in region A, and from the results of Fig. 2(a), if we picked data (0.5, 5) it would go to the limit cycle surrounding E_2 , and not to extinction. However, for $1 < x_1(0) < \frac{a_1}{b_1} = 5$, g_1 lies completely above $W^s(E_0)$, and below g_2 . In (c) however, g_1 dips below $W^s(E_0)$ even if $1 < x_1(0) < \frac{a_1}{b_1} = 5$. If one picked data (1.02, 7.4), it would not go to extinction, but to the limit cycle surrounding E_2 . All in all, there is a large range of initial data that we could pick above g_1 (but below g_2), s.t. trajectories initiating from that data, would go extinct in finite time.

responses such as Beddington–DeAngelis, ratio dependent, Crowley–Martin, Hassell–Varley and so on.

Lemma 4.3. Consider the predator–prey system given by (3). However, consider a predator functional response that depends on both the prey and predator $g(x_1, x_2) = w_0 \left(\frac{x_1}{x_1 + x_2 + d}\right)^{m_1}$. The solution $x_1(t)$ to the prey equation will go extinct in finite time, for initial conditions chosen s.t $1 \le x_1(0) \le \frac{a_1}{b_1}$, $f(x_1(0)) \le (x_2(0))^{m_2}$, where f is chosen via (31).

Proof. Consider the prey equation for initial condition $1 \le x_1(0) \le \frac{a_1}{b_1}$

$$\frac{dx_1}{dt} = a_1 x_1 - b_1 x_1^2 - w_0 \left(\frac{x_1}{x_1 + x_2 + d}\right)^{m_1} x_2^{m_2}
\leq a_1 x_1 - b_1 x_1^2 - w_0 \left(\frac{x_2^{m_2}}{\frac{a_1}{b_1} + d + x_2}\right)^{m_1} (x_1)^{m_1}
\leq a_1 x_1 - \frac{(x_2(0))^{m_2} e^{-m_2 a_2 t}}{w_0 (\frac{a_1}{b_1} + d + (x_2(0)) e^{(w_1 - a_2)t})^{m_1}} (x_1)^{m_1}$$
(30)

We now divide both sides by $(x_1)^{m_1}$, and follow [17] to attain that x_1 will go extinct in finite time as long as

$$(x_1(0))^{1-m_1} < \int_0^\infty \frac{(x_2(0))^{m_2} e^{-(m_2 a_2 + a_1(1-m_1))s}}{w_0(\frac{a_1}{b_1} + d + (x_2(0)) e^{(w_1 - a_2)s})^{m_1}} ds \quad \Box$$
 (31)

Remark 6. We leave the expression on the right hand side of (31) as an integral, depending on time, as the integral solved numerically does not yield a simple expression, but rather a complicated hyper-geometric function.

Corollary 1. Consider the predator–prey system given by (3), with a ratio-dependent, Crowley–Martin or Ivlev functional response. The solution $x_1(t)$ to the prey equation will go extinct in finite time, for appropriately chosen initial conditions.

Proof. The results of Lemma 4.3 apply to the ratio-dependent functional response trivially setting d=0, in the proof of the lemma. It would also apply to the Crowley–Martin functional response, where

 $g(x_1, x_2) = w_0 \left(\frac{x_1}{x_1 + x_2 + x_1 + x_2 + d}\right)^{m_1}$. Herein the key estimate would be,

$$-w_0 \left(\frac{x_2^{m_2}}{\frac{a_1}{b_1} + d + x_2 + x_1 x_2} \right)^{m_1}$$

$$\leq -w_0 \frac{(x_2(0))^{m_2} e^{-m_2 a_2 t}}{(\frac{a_1}{b_1} + d + (x_2(0))e^{(w_1 - a_2)t} + \frac{a_1}{b_1} (x_2(0))e^{(w_1 - a_2)t})^{m_1}}$$
(32)

thus yielding finite time extinction.

Also, note the Ivlev response, $g(x_1) = 1 - e^{-ax_1}$. Dividing by ϵx^l as in the proof of Theorem 4.2, works herein as well because, $\frac{e^{ax_1}}{\epsilon(x_1)^l(e^{ax_1}-1)}$ > 1, for appropriately chosen ϵ . In particular $\epsilon = \frac{1}{\frac{a_1}{h}}$, will suffice. \square

5. The effect of prey refuge

In the previous section it was shown that the prey population may go extinct in finite time. Therefore, we seek to investigate the effect of protecting the prey from predation with their habitat. The aim is to provided avenues for which the prey population will persist. Here, using similar ideas from [41], we introduce a prey refuge. A discussion of how a habitat controller may create a prey refuge is provided in section 7 of [41].

Essentially, one must protect a constant proportion of prey by replacing the predation term $g(x_1)$ by $g(rx_1)$, where $0 \le r \le 1$. Here, r is a refuge parameter, such that if r=0 then complete protection of the prey is provided while r=1 implies no protection and the original system (1) is recovered. Thus, we write the following system that models prey refuge as

$$\begin{cases} \frac{dx_1}{dt} &= a_1 x_1 - b_1 x_1^2 - w_2 \left(\frac{r x_1}{r x_1 + d}\right)^{m_1} x_2^{m_2}, \\ \frac{dx_2}{dt} &= -a_2 x_2 + w_3 \left(\frac{r x_1}{r x_1 + d}\right)^{m_1} x_2^{m_2}, \end{cases}$$
(33)

where w_2 is the maximum rate of per capita removal of prey and w_3 measures the efficiency of biomass conversion from prey to predator.

We now state our first result concerning prey refuge.

Theorem 5.1. Consider the predator–prey system given by (33). There exists a refuge $r^*(x_2(0), a_1, b_1, d, w_2, w_3, m_1, m_2) > 0$ and an interval $[y_1^*, y_2^*]$ s.t. for any $r < r^*$, and $x_1(0) \in [y_1^*, \infty)$ the solution $x_1(t)$ to the prey equation does not go extinct in finite time. In particular, $x_1(t)$ persists for all time, that is, $\liminf_{t\to\infty} x_1(t) \ge y_2^* > 0$.

Proof. From the second equation in (33),

$$\frac{dx_2}{dt} \le a_2 x_2 + w_3 x_2^{m_2}, \qquad t \ge 0.$$

We divide by $x_2^{m_2}$,

$$\frac{1}{1 - m_2} \frac{d}{dt} \left(x_2^{1 - m_2} \right) = x_2^{-m_2} \frac{dx_2}{dt} \le -a_2 x_2^{1 - m_2} + w_3$$

We integrate the above inequality using an integrating factor to obtain,

$$x_2^{1-m_2}(t) \le x_2^{1-m_2}(0)e^{-a(1-m_2)t} + \frac{w_3}{a_2} \left(1 - e^{-a(1-m_2)t}\right), \qquad t \ge 0.$$

This implies

$$x_2^{1-m_2}(t) \le \max\left\{x_2^{1-m_2}(0), \frac{w_3}{a_2}\right\}$$

and

$$x_2(t) \leq \max \left\{ x_2(0), \left(\frac{w_3}{a_2} \right)^{1/(1-m_2)} \right\}.$$

We substitute this inequality into the first equation of (33).

$$\frac{dx_1}{dt} \ge a_1x_1 - b_1x_1^2 - w_2 \left(\frac{rx_1}{rx_1 + d}\right)^{m_1} \alpha \left(x_2(0)\right)$$

where

$$\alpha\left(x_2(0)\right) = \max\left\{x_2^{m_2}(0), \left(\frac{w_3}{a_2}\right)^{m_2/(1-m_2)}\right\}.$$

We also have that

$$\frac{dx_1}{dt} \ge a_1 x_1 - b_1 x_1^2 - w_2 r^{m_1} x_1^{m_1} d^{-m_1} \alpha \left(x_2(0) \right).$$

By a comparison argument,

$$x_1(t) \ge y(t), \qquad t \ge 0 \tag{34}$$

where $y(0) = x_1(0)$ and

$$y' = a_1 y - b_1 y^2 - w_2 r^{m_1} y^{m_1} d^{-m_1} \alpha \left(x_2(0) \right). \tag{35}$$

We now analyze the scalar ODE (35). If the right hand side is strictly negative for all y > 0, no assertions can be made. So our goal is to show r > 0 can be chosen (small enough if required) such that the right hand side can be made positive, for certain ranges of initial data.

We next divide the right hand side by y,

$$\phi(y) = a_1 - b_1 y - r^{m_1} y^{m_1 - 1} \beta \left(x_2(0) \right).$$

where $\beta(x_2(0)) = w_2 d^{-m_1} \alpha(x_2(0))$.

We differentiate,

$$\phi'(y) = -b_1 + r^{m_1}(1 - m_1)y^{m_1 - 2}\beta\left(x_2(0)\right). \tag{36}$$

 ϕ attains a global maximum at $y^* > 0$ with $\phi'(y^*) = 0$,

$$y^* = \left(\frac{r^{m_1}(1 - m_1)\beta(x_2(0))}{b_1}\right)^{1/(2 - m_1)}.$$

Since $\phi'(y^*) = 0$, by (36), we obtain

$$y^* = r^{m_1/(2-m_1)} \left(\frac{(1-m_1)\beta(x_2(0))}{b_1} \right)^{1/(2-m_1)}.$$

thus we have that

$$\begin{split} \phi\left(y^*\right) &= a_1 - (2 - m_1) r^{m_1} r^{m_1(m_1 - 1)/(2 - m_1)} \\ &\left(\frac{(1 - m_1)\beta(x_2(0))}{b_1}\right)^{(m_1 - 1)/(2 - m_1)} \beta\left(x_2(0)\right) > 0, \end{split}$$

if,

$$r < \left[a_1 \left(\frac{1 - m_1}{b_1} \right)^{(1 - m_1)/(2 - m_1)} \beta(x_2(0))^{1/(m_1 - 2)} (2 - m_1)^{-1} \right]^{(2 - m_1)/m_1}$$

Now if $\phi(y^*) > 0$, by continuity of ϕ , it has two strictly positive zeros $0 < y_1^* < y^* < y_2^* < a_1/b_1$, which are equilibria of (35). y_1^* is a source and y_2^* is a sink.

The right hand side is strictly negative for $y \in (0, y_1^*)$ and $y \in (y_2^*, \infty)$ and strictly positive for $y \in (y_1^*, y_2^*)$. So any solution y of (35) with $y(0) > y_1^*$ satisfies $y(t) > y_1^*$ for all $t \ge 0$ and $y(t) \to y_2^*$ as $t \to \infty$. \square

We now state two conjectures concerning the effect of prey refuge on the overall dynamics of (33).

Conjecture 1. Assume that there exists no refuge, that is r=1, and $W^s(E_0)$ is below $W^u(E_1)$. One can introduce a refuge by decreasing r, to raise $W^s(E_0)$ whilst lowering $W^u(E_1)$. There exists a critical refuge r^* at which $W^s(E_0)$ meets $W^u(E_1)$ and a heteroclinic orbit is formed. In this case all trajectories go extinct. If trajectories start above the heteroclinic this occurs in finite time, and if below they approach the heteroclinic orbit, leading to eventual extinction in infinite time. For $r < r^*$, $W^s(E_0)$ will now lie above $W^u(E_1)$, and the interior equilibrium or limit cycle will be locally stable.

Conjecture 2. Assume that there exists no refuge, that is r = 1, and $W^{s}(E_{0})$ is above $W^{u}(E_{1})$, whilst E_{2} is unstable, surrounded by a unique stable limit cycle. One can introduce a refuge by decreasing r, that results in raising $W^s(E_0)$. There exists a critical refuge r^* at which E_2 becomes stable. Furthermore, there is a window of refugia $r \in [r^{**}, r^*]$, for which E_2 remains positive and stable. In this case all trajectories above $W^s(E_0)$ go extinct in finite time. If trajectories start below $W^s(E_0)$, they approach E_2 , and there is no extinction in finite time.

5.1. Bifurcation analysis

In this subsection, we analyze the qualitative changes in the dynamical behavior of model (33) under the effect of varying a specific parameter. The conditions and restrictions for the occurrence of saddlenode, Hopf, and transcritical bifurcations are derived. The classification is of codimension one bifurcations.

5.1.1. Saddle-node bifurcation

We investigate the possibility of saddle-node bifurcation of the positive interior equilibrium E_2 by using the intrinsic death rate of the predator population as a bifurcation parameter.

The following theorem states the restrictions for occurrence of a saddle-node bifurcation for model (33).

Theorem 5.2. The model (33) undergoes a saddle-node bifurcation around E_2 at a_2^* when the system parameters satisfy the restriction $\det(\mathbf{J}_r^*) =$ 0 along with the condition $\operatorname{tr}(\mathbf{J}_{\mathbf{r}}^*) < 0$.

5.1.2. Transcritical bifurcation

Here, we investigate the possibility of the existence of a transcritical bifurcation for the model (33). Transcritical bifurcation occurs when an equilibrium point interchanges its stability when it collides with another equilibrium point as a parameter is varied. The prey refuge parameter r is used as a bifurcation parameter.

The model (33) undergoes a transcritical bifurcation around $E_1(a_1/b_1,0)$ when the refuge r crosses the critical value of parameter

$$r_1^*$$
, where $w_3 > a_2$ and $r_1^* = \frac{b_1 d}{a_1} \left(\frac{a_1^{\frac{1}{m_1}}}{\frac{1}{m_1} - \frac{1}{m_1}} \right)$.

5.1.3. Hopf-bifurcation

We investigate the possibility of Hopf-bifurcation of the positive interior equilibrium E_2 by using the per capita rate of self-reproduction for the prey, a_1 as a bifurcation parameter. Then, the characteristic equation corresponding to model (33) at E_2 is given by

$$\lambda^2 + A_1(a_1)\lambda + B_1(a_1) = 0, (37)$$

where $A_1 = -\operatorname{tr}(\mathbf{J_r^*}) = -(b_{11} + b_{22})$ and $B_1 = \det(\mathbf{J_r^*}) = b_{11}b_{22} - b_{12}b_{21}$. The instability of model (33) is demonstrated via the following theorem by considering a_1 as a bifurcation parameter.

The model (33) undergoes a Hopf-bifurcation around Theorem 5.4. $E_2(x_1^*, x_2^*)$ when a_1 crosses some critical value of parameter a_1^* , where

$$\begin{split} a_1^* &= a_2 + 2b_1x_1^* + m_1w_2x_2^{*m_2} \left[\frac{r}{d + rx_1^*} - \frac{r^2x_1^*}{(rx_1^* + d)^2} \right] \left(\frac{rx_1^*}{rx_1^* + d} \right)^{m_1 - 1} \\ &- m_2w_3x_2^{*m_2 - 1} \left(\frac{rx_1^*}{rx_1^* + d} \right)^{m_1}, \end{split}$$

provided

(i)
$$A_1(a_1) = 0$$
,

(ii)
$$B_1(a_1) > 0$$
.

(ii)
$$B_1(a_1) > 0$$
,
(iii) $\frac{d}{da_1} \operatorname{Re} \lambda_i(a_1) \big|_{a_1 = a_1^*} \neq 0 \text{ at } a_1 = a_1^*, \ i = 1, 2.$

Theorem 5.5. The model (33) undergoes a Hopf-bifurcation around $E_2(x_1^*, x_2^*)$ when the refuge r crosses some critical value of parameter r_1^{**} provided

$$\begin{split} &(i) \ \ A_1(r)=0, \\ &(ii) \ \ B_1(r)>0, \\ &(iii) \ \ \frac{d}{dr} \ Re\lambda_i(r)\big|_{r=r_1^{**}} \neq 0 \ at \ r=r_1^{**}, \ i=1,2. \end{split}$$

Proof. The proof of Theorem 5.5 is similar to proof in Theorem 5.4 and omitted for brevity. \square

5.2. Numerical simulations

We perform numerical simulations of model (33) to verify some of our analytical results. For r = 0.3 and all other parameter values given in Table 2, the predator-free equilibrium point $E_1(9.52381,0)$ is a saddle and $E_2(4.83648, 9.52147)$ is locally asymptotically stable, see Fig. 7. By introducing a prey refuge of r = 0.3, we observed in Fig. 7(a) that $W^{s}(E_{0})$ is above $W^{u}(E_{1})$ as compared to Fig. 2(b) where $W^{s}(E_{0})$ is below $W^{u}(E_{1})$. Thus the stability of the interior equilibrium is altered and not all positive solutions tend towards E_0 .

In Fig. 7(b), $E_2(1.872, 6.0161)$ is unstable and we obtain a heteroclinic bifurcation when $W^{u}(E_1) = W^{s}(E_0)$ for 0.7750 < r < 0.7751.

The model undergoes Hopf-bifurcation around $E_2(3.32486, 2.59694)$ as the parameter r crosses its critical value $r_1^{**} = 0.43639$, see Fig. 8. The branch of periodic orbits bifurcation from r_1^{**} is stable and the first Lyapunov coefficient is $\sigma = -4.99384e^{-3}$, hence supercritical. Also, the model (33) undergoes transcritical bifurcation around $E_1(9.52381, 0)$ when the parameter r crosses its threshold $r_1^* = 0.15239$, see Fig. 8(a).

6. Discussions and conclusions

In this work, we consider a predator-prey model, that allows us to model both the feeding intensity of the predator, as well as the effect of mutual/predator interference. The model can also be seen as a model for an infectious disease that invades a susceptible population, causing persons infected by the disease to move from the susceptible class to infected. Various analytical guidelines are laid down to investigate the equilibria and possible bifurcations. These are challenging, as the functional responses considered are non-Lipschitz, and so solutions are non-unique. This however, provides the system with the interesting dynamic of finite time extinction of prey - followed by the infinite time extinction of the predator.

We consider this dynamic in detail. Theorem 4.1, shows that this is possible, using the Leibnitz transform $x_1 = \frac{1}{u}$, (say when $m_1 = 0.5$) for $x_0 \le \sqrt{\frac{w_0}{a_0}}$, and sufficiently large predator density $x_2(0)$. Theorem 4.1 is unable to quantify how large the predator density needs to be in terms of prey density, so as to achieve extinction. This quantification is very important for biocontrol applications — where it is important to know how many predators to release to drive a target pest/prey extinct [12]. Following [17], we are able to provide a stronger result via Theorem 4.2 — wherein an explicit curve, $x_2(0) = g_1(x_1(0))$ is provided, s.t, if one is above the curve then finite time extinction occurs for the prey x_1 . Note our result improves the results of [17], in lowering this curve, see Fig. 6.

This result is biologically important from a point of view of infectious disease modeling as well. It says that finite time extinction of the host (susceptible) population, is possible with fewer infected individuals than predicted by the threshold in [17]. Note our result, be it in the context of bio-control or infectious disease modeling, is not sharp. What is seen in numerical simulations is that the sharpest result would be if the curve $g_1(x_1(0)) = W^s(E_0)$, that is the stable manifold/separatrix of the extinction state, as seen in Fig. 6. However, an analytic expression of the stable manifold is often not explicitly possible — and bringing down $g_1(x_1(0))$ further, would be a worthwhile

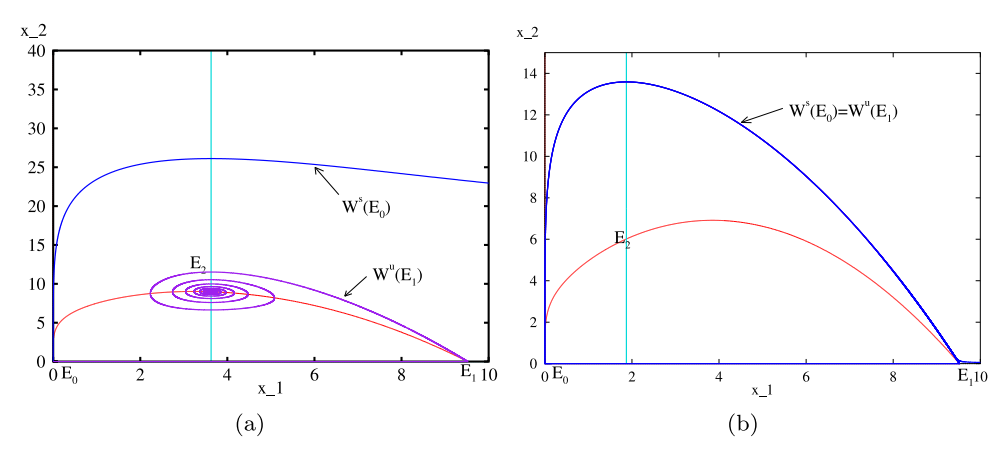


Fig. 7. (a) E_2 is locally asymptotically stable, $W^s(E_0)$ is above $W^u(E_1)$, and r = 0.3 (b) E_2 is unstable and $W^u(E_1) = W^s(E_0)$ when 0.7750 < r < 0.7751. Here $a_1 = 2$, $b_1 = 0.21$, and all other parameter sets are given in Table 2.

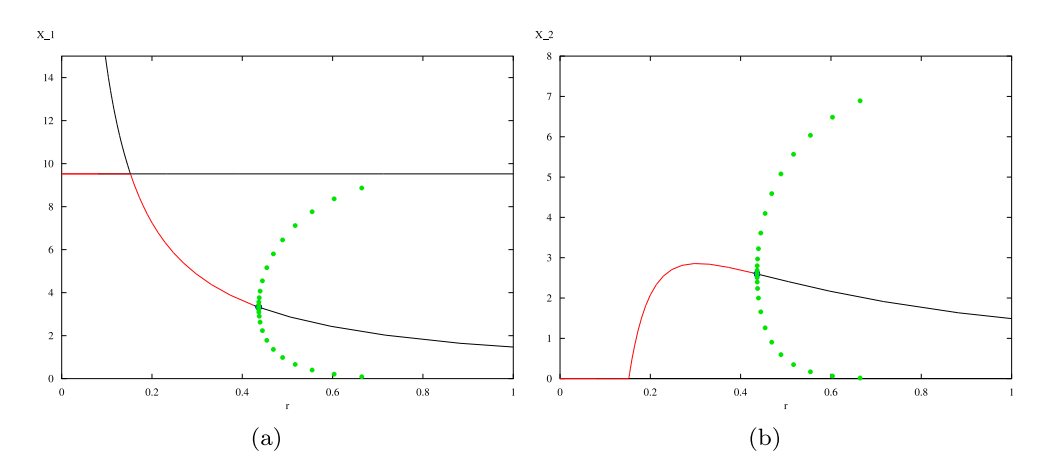


Fig. 8. Bifurcation diagrams of the model (33), as r crosses its critical values r_1^* and r_1^{**} . The stable and unstable interior equilibria are given by the lines in red and black, respectively. The solid circles (green) represent stable limit cycles. (a) prey (x_1) (b) predator (x_2) . Parameter sets are given in Table 2.

future direction of research. $W^s(E_0)$ may be unbounded in general, but numerics suggest otherwise — showing it to be bounded in the vertical direction, see Fig. 6. Another interesting future direction would be to consider an eco-epidemic model, such as in [50], where one can compare and contrast non-smooth disease dynamics with non-smooth dynamics in the predators functional response.

It is also important to note that our finite time extinction results, pertain to a much broader class of functional responses than the specific Holling type II form considered in (3). To this end please see Lemma 4.3 and Corollary 1. In particular our results are applicable to prey and predator dependent responses, such as of Beddington–DeAngelis and ratio dependent type. Through numerical simulations, it has been noticed that in the model (3), when $m_1 < 1$ and $m_2 = 1$, E_2 is not globally asymptotically stable (see Fig. 3(a)). We observe that the per capita rate of self-reproduction a_1 plays an important role because the interior equilibrium point E_2 changes stability at the bifurcation point e_1 (see Fig. 4). The limit cycle through the bifurcation point is stable hence a supercritical Hopf-bifurcation. This begets the question of stabilizing the interior equilibrium E_2 — to this end the effect of prey refuge is also considered in model (33).

Indeed it is observed that stability in the system can be maintained via provision of the prey with refuge. To the best of our knowledge our work is the first in the literature that brings this feature out in ecological systems, where finite time prey extinction is possible. This is rigorously established via Theorem 5.1. The requisite condition for a critical refuge, for persistence, derived via the theorem sheds light on various realistic ecological scenarios. The ecological validity of the prey extinction state $(0, x_2^*)$ is questionable. In the experiments of Gause [2],

once the prey has gone extinct the predator population also crashes, as there is no alternative/additional food in the experimental system. In a real scenario however, such a state might be indicative of a predator having switched to another food source after its primary source has depleted or surviving on additional food, such as in a bio-control situation [12]. Thus a possible future direction would be to consider models where the predator can also go extinct in finite time. The refuge result via Theorem 5.1 is important from an infectious disease modeling point as well. Numerical simulations show that protecting some proportion of the susceptible population (bringing in refuge) can always stabilize the endemic equilibrium. This has immense applications to epidemic control, such as the current COVID19 crisis [15], and is worthy of much future investigation. To these ends we conjecture that in any situation where $W^s(E_0)$ is below $W^u(E_1)$, one can introduce a refuge, so as to create a heteroclinic orbit. See Fig. 7(b). Also, we conjecture, based on numerical simulations, that if $W^{s}(E_0)$ is above $W^{u}(E_1)$, and E_2 is unstable, one can always introduce a refuge so as to stabilize E_2 . This strongly conforms with the experiments of Gause [2], where prey refuge is seen to be a factor that stabilizes populations.

The model possesses a rich array of dynamical behavior. We have established analytically the occurrence of various local bifurcations including saddle–node, transcritical and Hopf bifurcations. The occurrence of these local bifurcations is well supplemented with one parameter bifurcation diagrams (see Figs. 4, 5 and 8). Let us discuss the relevance of these findings to various ecological and epidemic contexts. If one observes Fig. 8, we see that for low refuge values $\approx 0.7 < r < 1$ (so if \approx a third or less of prey (host) population is protected) the interior equilibrium is unstable. Thus not much can be done dynamically to

stabilize populations, if government policy does not allow protection of about a third or more of the prey (host). When the refuge is increased to the regime $\approx 0.45 < r < 0.7$ we see stable population cycles. For $r \approx 0.43$, there is a Hopf-bifurcation and the interior equilibrium is stabilized. We see that the interior equilibrium remains stable (and predator free unstable) for the regime $\approx 0.15 < r < 0.43$. In the high refuge regime $\approx 0 < r < 0.15$, we see that the predator (disease) free equilibrium is stable. This tells us from an epidemic point of view that if one can protect 85% of the host or more, even under the effect of non-linear disease incidence, the disease free equilibrium can be stabilized. From a species conservation viewpoint (where one is attempting to conserve the prey) this tells us that if $\approx 0.15 < r < 0.43$ (or upwards of half the prey) is protected, we can maintain stable coexistence of predator-prey in the ecosystem. Once we increase this protection to 85% or more, one can maintain only prey in the ecosystem. This result is interesting – as the predator free equilibrium in most cases is a saddle.

Moreover, we observed that when $W^{s}(E_{0})$ is above $W^{u}(E_{1})$, all solutions with initial conditions above $W^s(E_0)$ goes to prey extinction in finite time (see Fig. 2(a)). Via numerical simulations, we obtained a heteroclinic bifurcation when $W^{u}(E_1) = W^{s}(E_0)$, where a limit cycle collides with the two saddle points E_0 and E_1 leading to a polycycle. This was conjectured in [51], but remained unproven or shown via numerical simulations — and is accomplished in the current manuscript. We observed that all solutions with initial conditions inside the polycycle except E_2 converge to the polycycle. Additionally, we noticed that all solutions with initial conditions outside the polycycle go to prey extinction in finite time (see Fig. 3(b)). These are in line with the result in [11]. Thus, from a practical point of view increasing m_1 or decreasing the feeding intensity of the predator, will maintain ecosystem balance, as this decreases the predator nullcline, decreasing predator numbers and increasing prey numbers.

All in all, the current work brings a new perspective in analyzing predator-prey as well as epidemic models, that permit the dynamic of finite time prey (host) population extinction. It quantifies the critical amount of refuge/protection for the prey (host) that can lead to population stabilization. This has large scale applications to biological control of pests and invasive species, epidemic control and conservation of endangered species, and will advance our understanding of these areas through continued current and future investigations, of the topics initiated herein.

Declaration of competing interest

The authors declare that they have no known competing financial interests or personal relationships that could have appeared to influence the work reported in this paper.

Acknowledgments

The authors would like to acknowledge valuable assistance by an anonymous referee in improving the overall quality of the manuscript, and greatly assisting with the proof of Theorem 5.1. RP and MB would like to acknowledge valuable partial support from the National Science Foundation via DMS 1839993 and DMS 1715044. KAF acknowledges the support received from Samford Faculty Development Grant (FUND 243084).

Appendix A

Proof of Theorem 3.3. To validate the restriction for the occurrence of saddle-node bifurcation, we apply Sotomayor's theorem [49] at $a_2 = a_2^*$. At $a_2 = a_2^*$, it can be seen that $\det(\mathbf{J}^*) = 0$ and $\operatorname{tr}(\mathbf{J}^*) < 0$ which indicates that the Jacobian (J^*) admits a zero eigenvalue. Let Uand V be the eigenvectors corresponding to the zero eigenvalue of the

matrix (\mathbf{J}^*) and $(\mathbf{J}^*)^T$ respectively. We obtain that $U = (u_1, u_2)^T$ and $V = (v_1, v_2)^T$, where $u_1 = -\frac{a_{12}^* u_2}{a_{11}^*}$, $v_1 = -\frac{a_{21}^* v_2}{a_{11}^*}$ and $u_2, v_2 \in \mathbb{R} \setminus \{0\}$. Furthermore, let $F = (F_1, F_2)^T$ and $X = (x_1^*, x_2^*)^T$, where F_1, F_2 are

$$F_1 = a_1 x_1 - b_1 x_1^2 - w_0 \left(\frac{x_1}{x_1 + d}\right)^{m_1} x_2^{m_2}$$

$$F_2 = -a_2 x_2 + w_1 \left(\frac{x_1}{x_1 + d}\right)^{m_1} x_2^{m_2}.$$

$$V^T F_{a_2}(X, a_2^*) = (v_1, v_2)(0, -x_2)^T = -v_2 x_2 \neq 0,$$

$$V^T [D^2 F(X, a_2^*)(U, U)] \neq 0.$$

Hence, from Sotomayor's theorem the model undergoes a saddle-node bifurcation around E_2 at $a_2 = a_2^*$. \square

Theorem A.1. The model (3) undergoes a saddle–node bifurcation around E_2 at w_1^* when the system parameters satisfy the restriction $\det(\mathbf{J}^*) = 0$ along with the condition $tr(J^*) < 0$.

Theorem A.2. The model (3) undergoes a saddle–node bifurcation around E_2 at w_0^* when the system parameters satisfy the restriction $\det(\mathbf{J}^*) = 0$ along with the condition $tr(J^*) < 0$.

Theorem A.3. The model (3) undergoes a saddle–node bifurcation around E_2 at b_1^* when the system parameters satisfy the restriction det $(\mathbf{J}^*) = 0$ along with the condition $tr(\mathbf{J}^*) < 0$.

Theorem A.4. The model (3) undergoes a saddle–node bifurcation around E_2 at a_1^* when the system parameters satisfy the restriction det $(\mathbf{J}^*) = 0$ along with the condition $tr(\mathbf{J}^*) < 0$.

Proof. The proof of Theorems A.1-A.4 are similar to the proof in Theorem 3.3 and omitted for brevity. □

Proof of Theorem 3.5. Clearly $A(a_1)$ and $B(a_1)$ are the smooth functions of a_1 . The roots of Eq. (12) are of the form $\lambda_1 = \zeta(a_1) + i\gamma(a_1)$ and $\lambda_2 = \zeta(a_1) - i\gamma(a_1)$ where $\zeta(a_1)$ and $\gamma(a_1)$ are real functions.

At $a_1 = a_1^*$, the characteristic equation (12) reduces to

$$\lambda^2 + B(a_1) = 0 {38}$$

By solving for the roots of Eq. (38), we obtain $\lambda_1 = i\sqrt{B}$ and $\lambda_2 = -i\sqrt{B}$. Hence a pair of purely imaginary eigenvalues. Furthermore, we validate the transversality condition:

$$\frac{d}{da_1} Re \lambda_i(a_1)|_{a_1 = a_1^*} \neq 0, i = 1, 2.$$

Substituting $\lambda(a_1) = \zeta(a_1) + i\gamma(a_1)$ into Eq. (12), we obtain

$$(\zeta(a_1) + i\gamma(a_1))^2 + A(a_1)(\zeta(a_1) + i\gamma(a_1)) + B(a_1) = 0.$$
(39)

Now, taking the derivative with respect to a_1 , we get

$$\begin{split} 2(\zeta(a_1) + i\gamma(a_1))(\dot{\zeta}(a_1) + i\dot{\gamma}(a_1)) + A(a_1)(\dot{\zeta}(a_1) + i\dot{\gamma}(a_1)) \\ + \dot{A}(a_1)(\zeta(a_1) + i\gamma(a_1)) + \dot{B}(a_1) &= 0. \end{split}$$

Separating the real and imaginary parts, we have

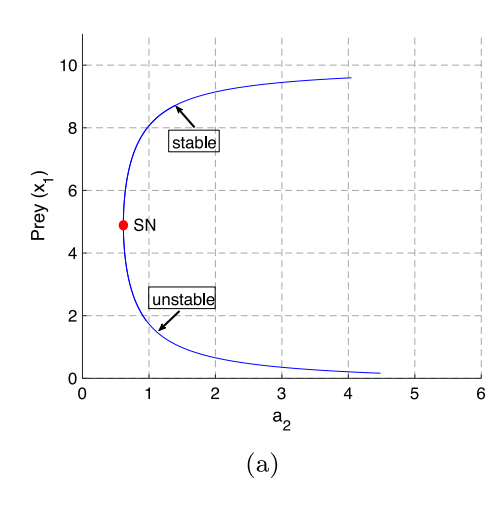
$$\dot{\zeta}(a_1)(2\zeta(a_1) + A(a_1)) + \dot{\gamma}(a_1)(-2\gamma(a_1)) + \dot{A}(a_1)\zeta(a_1) + \dot{B}(a_1) = 0,$$

which implies

$$\dot{\zeta}(a_1)Z_1(a_1) - \dot{\gamma}(a_1)Z_2(a_1) + Z_3(a_1) = 0, (40)$$

and

$$\dot{\zeta}(a_1)(2\gamma(a_1)) + \dot{\gamma}(a_1)(2\zeta(a_1) + A(a_1)) + \dot{A}(a_1)\gamma(a_1) = 0,$$



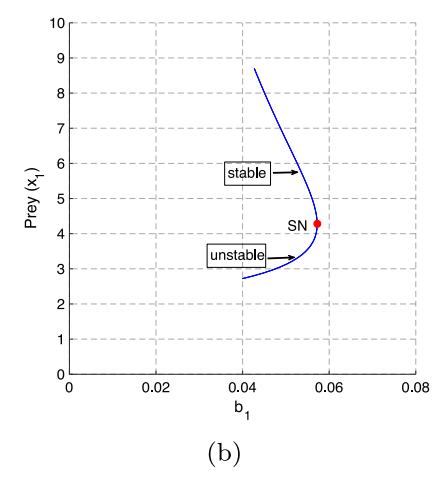


Fig. 9. Bifurcation diagrams illustrating (a) SN at $a_2 = a_2^* = 0.61515$ (b) SN at $b_1 = b_1^* = 0.05722$. Other parameter sets are given in Table 3. (SN: Saddle-node bifurcation.)

which implies

$$\dot{\zeta}(a_1)Z_2(a_1) + \dot{\gamma}(a_1)Z_1(a_1) + Z_4(a_1) = 0, (41)$$

where $Z_1(a_1) = 2\zeta(a_1) + A(a_1)$, $Z_2(a_1) = 2\gamma(a_1)$, $Z_3(a_1) = \dot{A}(a_1)\zeta(a_1) + \dot{B}(a_1)$ and $Z_4(a_1) = \dot{A}(a_1)\gamma(a_1)$.

Multiplying equation (49) by $Z_1(a_1)$ and Eq. (50) by $Z_2(a_1)$ and then adding them, we obtain

$$(Z_1^2(a_1) + Z_2^2(a_1))\dot{\zeta}(a_1) + Z_1(a_1)Z_3(a_1) + Z_2(a_1)Z_4(a_1) = 0, \tag{42}$$

thus solving for $\dot{\zeta}(a_1)$ from Eq. (51) and at $a_1 = a_1^*$,

$$\frac{d}{da_1} \operatorname{Re} \lambda_i(a_1)|_{a_1=a_1^*} = \dot{\zeta}(a_1^*) = \frac{-\left[Z_1(a_1^*)Z_3(a_1^*) + Z_2(a_1^*)Z_4(a_1^*)\right]}{Z_1^2(a_1^*) + Z_2^2(a_1^*)}.$$

It is easy to verify that $Z_1(a_1^*)Z_3(a_1^*) + Z_2(a_1^*)Z_4(a_1^*) \neq 0$ and $Z_1^2(a_1^*) + Z_2^2(a_1^*) \neq 0$ which implies $\frac{d}{da_1}Re\lambda_i(a_1)|_{a_1=a_1^*} \neq 0$. Hence, a Hopf-bifurcation occurs around $E_2(x_1^*, x_2^*)$ at $a_1 = a_1^*$. \square

Appendix B

B.1. Existence of equilibria and analytic guidelines

Similar to Section 3, we investigate and analyze the equilibrium solutions of our mathematical model with prey refuge. Consider the steady state equations of (33):

$$a_1 x_1 - b_1 x_1^2 - w_2 \left(\frac{r x_1}{r x_1 + d}\right)^{m_1} x_2^{m_2} = 0$$

$$(43)$$

$$-a_2x_2 + w_3 \left(\frac{rx_1}{rx_1 + d}\right)^{m_1} x_2^{m_2} = 0$$
 (44)

The above equations (43) and (44) have three types of non-negative equilibria:

- (i) The trivial equilibrium $E_0(0,0)$.
- (ii) The predator-free equilibrium $E_1(a_1/b_1, 0)$.
- (iii) The interior equilibrium $E_2(x_1^*, x_2^*)$ where x_1^* and x_2^* are related by

$$x_2^* = \frac{w_3}{w_2 a_2} \left[a_1 x_1^* - b_1 x_1^{*2} \right].$$

The variational matrix $\mathbf{J}^*_{\mathbf{r}}$ of the model (33) around any of the possible interior equilibria $E_2(x_1^*,x_2^*)$ is

$$\mathbf{J}_{\mathbf{r}}^* = \begin{bmatrix} b_{11} & b_{12} \\ b_{21} & b_{22} \end{bmatrix}.$$

where

$$b_{11} = a_1 - 2b_1 x_1^* - m_1 w_2 x_2^{*m_2} \left[\frac{r}{d + r x_1^*} - \frac{r^2 x_1^*}{(r x_1^* + d)^2} \right] \left(\frac{r x_1^*}{r x_1^* + d} \right)^{m_1 - 1},$$

$$m_2 w_2 x_2^{*m_2 - 1} (r x_1^*)^{m_1}$$

$$b_{12} = -\frac{m_2 w_2 x_2^{*m_2 - 1} (r x_1^*)^{m_1}}{(r x_1^* + d)^{m_1}},$$

$$b_{21} = m_1 d w_3 r^{m_1} x_2^{*m_2} \left(\frac{x_1^{*m_1 - 1}}{(r x_1^* + d)^{m_1 + 1}}\right),$$

$$b_{22} = -a_2 + m_2 w_3 x_2^{*m_2 - 1} \left(\frac{r x_1^*}{r x_1^* + d} \right)^{m_1}.$$

The characteristic equation corresponding to J_{π}^* is given by

$$\lambda^2 - \operatorname{tr}(\mathbf{J}_{\mathbf{r}}^*)\lambda + \det(\mathbf{J}_{\mathbf{r}}^*) = 0,$$

where

$$\begin{split} \operatorname{tr}\left(\mathbf{J}_{\mathbf{r}}^{*}\right) &= b_{11} + b_{22} \\ &= a_{1} - a_{2} - 2b_{1}x_{1}^{*} - m_{1}w_{2}x_{2}^{*m_{2}} \\ &\times \left[\frac{r}{d + rx_{1}^{*}} - \frac{r^{2}x_{1}^{*}}{(rx_{1}^{*} + d)^{2}}\right] \left(\frac{rx_{1}^{*}}{rx_{1}^{*} + d}\right)^{m_{1} - 1} \\ &+ m_{2}w_{3}x_{2}^{*m_{2} - 1} \left(\frac{rx_{1}^{*}}{rx_{1}^{*} + d}\right)^{m_{1}}, \end{split}$$

and

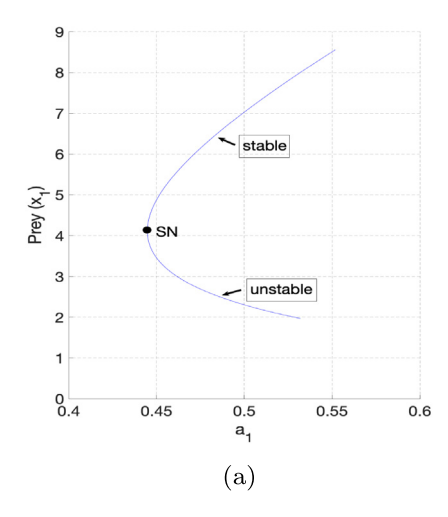
$$\begin{split} \det{(\mathbf{J_r^*})} &= b_{11}b_{22} - b_{12}b_{21} \\ &= \left(a_1 - 2b_1x_1^* - m_1w_2x_2^{*m_2} \left[\frac{r}{d + rx_1^*} - \frac{r^2x_1^*}{(rx_1^* + d)^2}\right] \left(\frac{rx_1^*}{rx_1^* + d}\right)^{m_1 - 1}\right) \\ &\times \left(-a_2 + m_2w_3x_2^{*m_2 - 1} \left(\frac{rx_1^*}{rx_1^* + d}\right)^{m_1}\right) \\ &- \left(-\frac{m_2w_2x_2^{*m_2 - 1} (rx_1^*)^{m_1}}{(rx_1^* + d)^{m_1}}\right) \left(m_1dw_3r^{m_1}x_2^{*m_2} \left(\frac{x_1^{*m_1 - 1}}{(rx_1^* + d)^{m_1 + 1}}\right)\right). \end{split}$$

Here, $\operatorname{tr}(\mathbf{J}_{\mathbf{r}}^*)$ and $\det(\mathbf{J}_{\mathbf{r}}^*)$ represent the trace and determinant of the variational matrix. Hence the stability of $E_2(x_1^*, x_2^*)$ is determined by the sign of $\det(\mathbf{J}_{\mathbf{r}}^*)$ and $\operatorname{tr}(\mathbf{J}_{\mathbf{r}}^*)$.

The above results are summarized in the following theorem.

Theorem B.1. The interior equilibrium $E_2(x_1^*, x_2^*)$ of system (33) is locally asymptotically stable if $\operatorname{tr}(\mathbf{J}_{\mathbf{r}}^*) < 0$ and $\det(\mathbf{J}_{\mathbf{r}}^*) > 0$ by Routh–Hurwitz stability criteria.

Proof. The proof follows directly from the above discussion and hence omitted for brevity. □



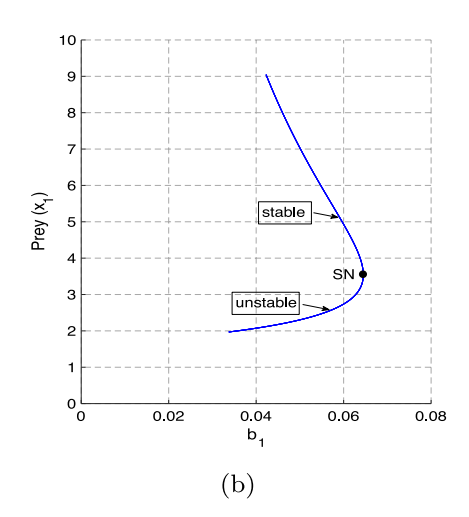


Fig. 10. Bifurcation diagrams of the model (33) illustrating (a) SN at $a_1 = a_1^* = 0.44476$, (b) SN at $b_1 = b_1^* = 0.064498$. Here r = 0.3 and other parameter sets are given in Table 3. (SN: Saddle-node bifurcation.)

Remark 7. When r = 1, we recover the det (\mathbf{J}^*) and tr (\mathbf{J}^*) for Section 3 where $w_2 = w_0$ and $w_3 = w_1$.

Proof of Theorem 5.2. To validate the restriction for the occurrence of saddle-node bifurcation, we apply Sotomayor's theorem [49] at $a_2=a_2^*$. At $a_2=a_2^*$, it can be seen that $\det(\mathbf{J_r^*})=0$ and $\operatorname{tr}(\mathbf{J_r^*})<0$ which indicates that the Jacobian $(\mathbf{J_r^*})$ admits a zero eigenvalue. Let U and V be the eigenvectors corresponding to the zero eigenvalue of the matrix $(\mathbf{J_r^*})$ and $(\mathbf{J_r^*})^T$ respectively. We obtain that $U=(u_1,u_2)^T$ and $V=(v_1,v_2)^T$, where $u_1=-\frac{b_{12}^*u_2}{b_{11}^*}$, $v_1=-\frac{b_{21}^*v_2}{b_{11}^*}$ and $u_2,v_2\in\mathbb{R}\setminus\{0\}$. Let $G=(G_1,G_2)^T$ and $X=(x_1^*,x_2^*)^T$, where G_1,G_2 are given by

$$G_1 = a_1 x_1 - b_1 x_1^2 - w_2 \left(\frac{r x_1}{r x_1 + d}\right)^{m_1} x_2^{m_2},\tag{45}$$

$$G_2 = -a_2 x_2 + w_3 \left(\frac{r x_1}{r x_1 + d}\right)^{m_1} x_2^{m_2}. \tag{46}$$

Now

$$V^T G_{a_2}(X, a_2^*) = (v_1, v_2)(0, -x_2)^T = -v_2 x_2 \neq 0,$$

and

$$V^{T}[D^{2}G(X, a_{2}^{*})(U, U)] \neq 0.$$

Hence from Sotomayor's theorem the model (33) undergoes a saddle-node bifurcation around E_2 at $a_2 = a_2^*$. \square

Theorem B.2. The model (33) undergoes a saddle–node bifurcation around E_2 at w_3^* when the system parameters satisfy the restriction $\det(\mathbf{J_r^*}) = 0$ along with the condition $\operatorname{tr}(\mathbf{J_r^*}) < 0$.

Theorem B.3. The model (33) undergoes a saddle-node bifurcation around E_2 at w_2^* when the system parameters satisfy the restriction $\det(\mathbf{J_r^*}) = 0$ along with the condition $\operatorname{tr}(\mathbf{J_r^*}) < 0$.

Theorem B.4. The model (33) undergoes a saddle–node bifurcation around E_2 at b_1^* when the system parameters satisfy the restriction $\det(\mathbf{J_r^*}) = 0$ along with the condition $\operatorname{tr}(\mathbf{J_r^*}) < 0$.

Theorem B.5. The model (33) undergoes a saddle–node bifurcation around E_2 at a_1^* when the system parameters satisfy the restriction $\det(\mathbf{J_r^*}) = 0$ along with the condition $\operatorname{tr}(\mathbf{J_r^*}) < 0$.

Proof. The proof of Theorems B.2–B.5 are similar to the proof in Theorem 5.2 and omitted for brevity. \Box

Proof of Theorem 5.3. The variational matrix $\mathbf{J}_{\mathbf{r}_1^*}$ of the model (33) for $0 < m_1 < 1$ and $m_2 = 1$ evaluated at $r = r_1^*$ around the predator-free equilibrium $E_1(a_1/b_1, 0)$ is given by

$$\mathbf{J}_{\mathbf{r_1}}^* = \begin{bmatrix} -a_1 & -w_2 \left(\frac{r_1^* a_1}{r_1^* a_1 + b_1 d} \right)^{m_1} \\ 0 & 0 \end{bmatrix}.$$

At $r=r_1^*$, the matrix $\mathbf{J}_{\mathbf{r}_1^*}$ has a negative eigenvalue and a zero eigenvalue. Let U and V be the eigenvectors corresponding to the zero eigenvalue of the matrix $(\mathbf{J}_{\mathbf{l}_{\mathbf{r}^*}})$ and $(\mathbf{J}_{\mathbf{r}^*})^T$ respectively. Then

$$U = \left(1, -\frac{a_1}{w_2} \left(1 + \frac{b_1 d}{r_1^* a_1}\right)^{m_1}\right)^T, \qquad V = (0, 1)^T.$$

Let $G = (G_1, G_2)^T$ and $X = (a_1/b_1, 0)^T$, where G_1, G_2 are defined in (45) and (46). Now we have

$$V^T G_r(X, r_1^*) = (0, 1)(0, 0)^T = 0,$$

additionally

$$V^T \left[DG_r(X, r_1^*) U \right] \neq 0$$

and

$$V^T\left[D^2G(X,r_1^*)(U,U)\right]\neq 0.$$

Hence using Sotomayor's theorem the model (33) undergoes a transcritical bifurcation around E_1 when the refuge r crosses the critical value of the parameter r_1^* . \square

Proof of Theorem 5.4. Clearly $A_1(a_1)$ and $B_1(a_1)$ are the smooth functions of a_1 . The roots of Eq. (37) are of the form $\lambda_1 = \theta(a_1) + i\varpi(a_1)$ and $\lambda_2 = \theta(a_1) - i\varpi(a_1)$ where $\theta(a_1)$ and $\varpi(a_1)$ are real functions.

At $a_1 = a_1^*$, the characteristic equation (37) reduces to

$$\lambda^2 + B_1(a_1) = 0 (47)$$

By solving for the roots of Eq. (47), we obtain $\lambda_1 = i\sqrt{B_1}$ and $\lambda_2 = -i\sqrt{B_1}$. Therefore, we have purely imaginary eigenvalues. Hence, we are left with validating the transversality condition. Namely,

$$\frac{d}{da_1} Re \lambda_i(a_1)|_{a_1 = a_1^*} \neq 0, i = 1, 2.$$

Substituting $\lambda(a_1) = \vartheta(a_1) + i\varpi(a_1)$ into Eq. (37), we obtain

$$(\vartheta(a_1) + i\varpi(a_1))^2 + A_1(a_1)(\vartheta(a_1) + i\varpi(a_1)) + B_1(a_1) = 0.$$
(48)

Upon taking the derivative with respect to a_1 we obtain:

$$2(\vartheta(a_1)+i\varpi(a_1))(\dot{\vartheta}(a_1)+i\dot{\varpi}(a_1))+A_1(a_1)(\dot{\vartheta}(a_1)+i\dot{\varpi}(a_1))$$

$$+\dot{A}_1(a_1)(\vartheta(a_1)+i\varpi(a_1))+\dot{B}_1(a_1)=0.$$

Separating the real and imaginary parts, we have

$$\dot{\vartheta}(a_1)(2\vartheta(a_1) + A_1(a_1)) + \dot{\varpi}(a_1)(-2\varpi(a_1)) + \dot{A}_1(a_1)\vartheta(a_1) + \dot{B}_1(a_1) = 0,$$

which implies

$$\dot{\vartheta}(a_1)Z_1(a_1) - \dot{\varpi}(a_1)Z_2(a_1) + Z_3(a_1) = 0, (49)$$

and

$$\dot{\vartheta}(a_1)(2\varpi(a_1)) + \dot{\varpi}(a_1)(2\vartheta(a_1) + A_1(a_1)) + \dot{A}_1(a_1)\varpi(a_1) = 0,$$

which implies

$$\dot{\vartheta}(a_1)Z_2(a_1) + \dot{\varpi}(a_1)Z_1(a_1) + Z_4(a_1) = 0, \tag{50}$$

where $Z_1(a_1) = 2\vartheta(a_1) + A_1(a_1)$, $Z_2(a_1) = 2\varpi(a_1)$, $Z_3(a_1) = A_1(a_1)\vartheta(a_1) + B_1(a_1)$ and $Z_4(a_1) = A_1(a_1)\varpi(a_1)$. Multiplying equation (49) by $Z_1(a_1)$ and Eq. (50) by $Z_2(a_1)$ and then adding them, we obtain

$$(Z_1^2(a_1) + Z_2^2(a_1))\dot{\theta}(a_1) + Z_1(a_1)Z_3(a_1) + Z_2(a_1)Z_4(a_1) = 0,$$
 (51)

thus solving for $\dot{\vartheta}(a_1)$ from Eq. (51) and at $a_1 = a_1^*$,

$$\frac{d}{da_1} \operatorname{Re} \lambda_i(a_1) \big|_{a_1 = a_1^*} = \dot{\vartheta}(a_1^*) = \frac{-\left[Z_1(a_1^*) Z_3(a_1^*) + Z_2(a_1^*) Z_4(a_1^*) \right]}{Z_1^2(a_1^*) + Z_2^2(a_1^*)}.$$

It is easy to verify that $Z_1(a_1^*)Z_3(a_1^*) + Z_2(a_1^*)Z_4(a_1^*) \neq 0$ and $Z_1^2(a_1^*) + Z_2^2(a_1^*) \neq 0$ which implies $\frac{d}{da_1} Re \lambda_i(a_1)|_{a_1=a_1^*} \neq 0$. Hence, a Hopf-bifurcation occurs around $E_2(x_1^*, x_2^*)$ at $a_1 = a_1^*$. \square

References

- J.R. Beddington, Mutual interference between parasites or predators and its effect on searching efficiency, J. Animal. Ecol. 44 (1975) 331–340.
- [2] G.F. Gause, The Struggle for Existence, Williams & Wilkins, Baltimore, Maryland, USA, 1934.
- [3] C.S. Holling, The components of predation as revealed by a study of small mammal predation of the European pine sawfly, Canad. Entomol. 91 (1959)
- [4] A.J. Lotka, Elements of Physical Biology, Williams and Wilkins, Baltimore, 1925, Reprinted as Elements of mathematical biology, Dover, New York.
- [5] Y. Kuang, Some mechanistically derived population models, Math. Biosci. Eng. 4 (4) (2007) 1–11.
- [6] J. Sugie, R. Kohno, R. Miyazaki, On a predator–prey system of holling type, Proc. Amer. Math. Soc. 125 (7) (1997) 2041–2050.
- [7] J. Sugie, M. Katayama, Global asymptotic stability of a predator-prey system of holling type, Nonlinear Anal. Theor. 38 (1) (1999) 105-121.
- [8] P.A. Braza, Predator-prey dynamics with square root functional responses, Nonlinear Anal. RWA 13 (4) (2012) 1837–1843.
- [9] M.R. Myerscough, M.J. Darwen, W.L. Hogarth, Stability, persistence and structural stability in a classical predator-prey model, Ecol. Model. 89 (1-3) (1996)
- [10] Christos C. Ioannou, Graeme D. Ruxton, Jens Krause, Search rate, attack probability, and the relationship between prey density and prey encounter rate, Behav. Ecol. 19 (4) (2008) 842–846, http://dx.doi.org/10.1093/beheco/arn038; Bull. Math. Biol. 73 (10) (2011) 2249-2276.
- [11] N. Beroual, T. Sari, A predator-prey system with holling-type functional response, Proc. Amer. Math. Soc. (2020) http://dx.doi.org/10.1090/proc/15166.
- [12] R.D. Parshad, S. Wickramsooriya, S. Bailey, A remark on Biological control through provision of additional food to predators: A theoretical study[Theor. Popul. Biol. 72 (2007) 111–120], Theoret. Popul. Biol. (2019).
- [13] D.W. Ragsdale, D.A. Landis, J. Brodeur, G.E. Heimpel, N. Desneux, Ecology and management of the soybean aphid in North America, Ann. Rev. Entomol. 56 (2011) 375–399.
- [14] M.E. O'Neal, A.J. Varenhorst, M.C. Kaiser, Rapid evolution to host plant resistance by an invasive herbivore: soybean aphid (aphis glycines) virulence in north america to aphid resistant cultivars, Current Opin. Insect Sci. 26 (2018)
- [15] P. Mehta, D.F. McAuley, M. Brown, E. Sanchez, R.S. Tattersall, J.J. Manson, COVID-19: consider cytokine storm syndromes and immunosuppression, Lancet 395 (10229) (2020) 1033–1034.
- [16] A. Farrell, Prey-Predator-Parasite: An Ecosystem Model with Fragile Persistence, Arizona State University, 2017.
- [17] A.P. Farrell, J.P. Collins, A.L. Greer, H.R. Thieme, Do fatal infectious diseases eradicate host species?, J. Math. Biol. 77 (6–7) (2018) 2103–2164.
- [18] A.P. Farrell, J.P. Collins, A.L. Greer, H.R. Thieme, Times from infection to disease-induced death and their influence on final population sizes after epidemic outbreaks, Bull. Math. Biol. 80 (7) (2018) 1937–1961.

- [19] A.L. Greer, C.J. Briggs, J.P. Collins, Testing a key assumption of host-pathogen theory: Density and disease transmission, Oikos 117 (11) (2008) 1667–1673.
- [20] A. Fenton, J.P. Fairbairn, R. Norman, P.J. Hudson, Parasite transmission: reconciling theory and reality, J. Anim. Ecol. 71 (5) (2002) 893–905.
- [21] G. Dwyer, J.S. Elkinton, J.P. Buonaccorsi, Host heterogeneity in susceptibility and disease dynamics: tests of a mathematical model, Amer. Nat. 150 (6) (1997) 685–707
- [22] R.P. Gupta, P. Chandra, Bifurcation analysis of modified Leslie–Gower predator–prey model with Michaelis–Menten type prey harvesting, J. Math. Anal. Appl. 398 (1) (2013) 278–295.
- [23] F.M. Hilker, M. Langlais, H. Malchow, The Allee effect and infectious diseases: extinction, multistability, and the (dis-) appearance of oscillations, Amer. Nat. 173 (1) (2009) 72–88.
- [24] E. González-Olivares, A. Rojas-Palma, Allee effect in gause type predator-prey models: Existence of multiple attractors, limit cycles and separatrix curves, A Brief Rev. Math. Model. Natural Phenomena 8 (6) (2013) 143–164.
- [25] A. Friedman, A.A. Yakubu, Fatal disease and demographic Allee effect: population persistence and extinction, J. Biol. Dyn. 6 (2) (2012) 495–508.
- [26] H.R. Thieme, T. Dhirasakdanon, Z. Han, R. Trevino, Species decline and extinction: synergy of infectious disease and Allee effect?, J. Biol. Dyn. 3 (2-3) (2009) 305–323.
- [27] M. Hassell, Mutual interference between searching insect parasites, J. Anim. Ecol. 40 (1971) 473–486.
- [28] M. Hassell, Density dependence in single species population, J. Anim. Ecol. 44 (1975) 283–295.
- [29] D.L. DeAngelis, R.A. Goldstein, R.V. ONeill, A model for trophic interaction, Ecology 56 (1975) 881–892.
- [30] H.I. Freedman, Stability analysis of a predator-prey system with mutual interference and density-dependent death rates, Bull. Math. Biol. 41 (1) (1979) 67-78.
- [31] A.D. Bazykin, Nonlinear dynamics of interacting populations, 1998.
- [32] R. Arditi, J.M. Callois, Y. Tyutyunov, C. Jost, Does mutual interference always stabilize predator–prey dynamics? A comparison of models, C. R. Biol. 327 (11) (2004) 1037–1057.
- [33] L.H. Erbe, H.I. Freedman, Modeling persistence and mutual interference among subpopulations of ecological communities, Bull. Math. Biol. 47 (2) (1985) 295–304
- [34] J.P. DeLong, D.A. Vasseur, Mutual interference is common and mostly intermediate in magnitude, BMC Ecol. 11 (1) (2011).
- [35] R.K. Upadhyay, V.S.H. Rao, Short-term recurrent chaos and role of Toxin Producing Phytoplankton (TPP) on chaotic dynamics in aquatic systems, Chaos Solitons Fractals 39 (4) (2009) 1550–1564.
- [36] H.W. McKenzie, E.H. Merrill, R.J. Spiteri, M.A. Lewis, How linear features alter predator movement and the functional response, Interface focus 2 (2) (2012) 205–216.
- [37] C.M. Mols, K. van Oers, L.M. Witjes, C.M. Lessells, P.J. Drent, M.E. Visser, Central assumptions of predator-prey models fail in a semi-natural experimental system, Proc. R. Soc. Lond. Ser. B: Biol. Sci. 271 (Suppl. 3) (2004) S85–S87.
- [38] G.D. Ruxton, Increasing search rate over time may cause a slower than expected increase in prey encounter rate with increasing prey density, Biol. Lett. 1 (2) (2005) 133–135.
- [39] T.K. Kar, Stability analysis of a prey-predator model incorporating a prey refuge, Commun. Nonlinear Sci. Numer. Simul. 10 (6) (2005) 681–691.
- [40] D.L. Finke, R.F. Denno, Spatial refuge from intraguild predation: implications for prev suppression and trophic cascades. Oecologia 149 (2) (2006) 265–275.
- [41] R.D. Parshad, E. Quansah, K. Black, M. Beauregard, Biological control via ecological damping: an approach that attenuates non-target effects, Math. Biosci. 273, 23–44.
- [42] V. Křivan, On the Gause predator-prey model with a refuge: a fresh look at the history, J. Theoret. Biol. 274 (1) (2011) 67–73.
- [43] K. Wang, Y. Zhu, Periodic solutions, permanence and global attractivity of a delayed impulsive prey-predator system with mutual interference, Nonlinear Analysis RWA 14 (2) (2013) 1044–1054.
- [44] R.K. Upadhyay, R. Agrawal, Modeling the effect of mutual interference in a delay-induced predator-prey system, J. Appl. Math. Comput. 49 (2015) 13–39.
- [45] R.K. Upadhyay, R. Parshad, K. Antwi-Fordjour, E. Quansah, S. Kumari, Global dynamics of stochastic predator–prey with mutual interference and prey defense, J. Appl. Math. Comput. 60 (2019) 169–190.
- [46] J.D. Murray, Mathematical Biology, Springer, New York, 1993.
- [47] A. Dhooge, W. Govaerts, Yu. A. Kuznetsov, H.G.E. Meijer, B. Sautois, New features of the software matcont for bifurcation analysis of dynamical systems, MCMDS 14 (2) (2009) 147–175.
- [48] B. Ermentrout, Simulating, Analyzing, and Animating Dynamical Systems: A Guide to XPPAUT for Researchers and Students, vol. 14, SIAM, 2002.
- [49] L. Perko, Differential Equations and Dynamical Systems, vol. 7, Springer Science & Business Media, 2013.
- [50] F.M. Hilker, K. Schmitz, Disease-induced stabilization of predator-prey oscillations, J. Theoret. Biol. 255 (3) (2008) 299–306.
- [51] N. Beroual, A. Bendjeddou, On a Predator–Prey System with Holling Functional Response: x p/(a+ x p), Natl. Acad. Sci. Lett. 39 (1) (2016) 43–46.